Modeling of Tool-Tissue Interactions for Computer-Based Surgical Simulation: A Literature Review

Sarthak Misra, **K. T. Ramesh**, and **Allison M. Okamura**
Department of Mechanical Engineering, The Johns Hopkins University

Abstract

Surgical simulators present a safe and potentially effective method for surgical training, and can also be used in robot-assisted surgery for pre- and intra-operative planning. Accurate modeling of the interaction between surgical instruments and organs has been recognized as a key requirement in the development of high-fidelity surgical simulators. Researchers have attempted to model tool-tissue interactions in a wide variety of ways, which can be broadly classified as (1) linear elasticity-based, (2) nonlinear (hyperelastic) elasticity-based finite element (FE) methods, and (3) other techniques that not based on FE methods or continuum mechanics. Realistic modeling of organ deformation requires populating the model with real tissue data (which are difficult to acquire *in vivo*) and simulating organ response in real time (which is computationally expensive). Further, it is challenging to account for connective tissue supporting the organ, friction, and topological changes resulting from tool-tissue interactions during invasive surgical procedures. Overcoming such obstacles will not only help us to model tool-tissue interactions in real time, but also enable realistic force feedback to the user during surgical simulation. This review paper classifies the existing research on tool-tissue interactions for surgical simulators specifically based on the modeling techniques employed and the kind of surgical operation being simulated, in order to inform and motivate future research on improved tool-tissue interaction models.

1. Introduction

People have always sought ways to understand and model the structure and functions of the human body. The earliest known anatomical models used for surgical planning were recorded around 800 B.C. in India for the procedure of rhinoplasty, in which a flap of skin from the forehead is used to reconstruct a nose. These ancient practitioners used leaves to represent three-dimensional flexible tissues and plan the surgical operation (Carpue, 1981). Before the advent of medical imaging a century ago, the only practical way to see inside the human body was to observe an operation or by dissection. However, cultural and religious beliefs, the difficulty of obtaining cadavers, and lack of refrigeration imposed restrictions on the widespread use of dissection. Frustrated by these limitations, Louis Thomas Jerôme Auzoux, a 19th century French physician, improved and popularized anatomical papier mâché models (Davis, 1975). By the early 20th century, inexpensive and realistic plastic anatomical models that could be assembled and painted became popular with medical students. Though human cadavers and animals, however, are still used for training and, in some cases, surgical planning.

In the past decade, advances in computer hardware and software, and use of high-fidelity graphics have made it possible to create simulations of medical procedures. Computer-based surgical simulation provides an efficient, safe, and ethical method for training clinicians by

Corresponding Author: Allison M. Okamura, 125 Computational Science and Engineering Building, Department of Mechanical Engineering, The Johns Hopkins University, 3400 North Charles Street, Baltimore, MD 21218 USA, e-mail: aokamura@jhu.edu.

emphasizing the user's real-time interaction with medical instruments, surgical techniques, and realistic organ models that are anatomically and physiologically accurate. The objective is to create models that support medical practitioners by allowing them to visualize, feel, and be fully immersed in a realistic environment. This implies that the simulator must not only accurately represent the anatomical details and deformation of the organ, but also feed back realistic tool-tissue interaction forces to the user. As an example, consider the prototype hysteroscopy training simulator shown in Figure 1, which was developed at Eidgenössische Technische Hochschule (ETH) Zürich (Harders et al., 2006). This surgical simulator allows real-time visualization of the surgical procedure along with force feedback to the user.

The development of realistic surgical simulation systems requires accurate modeling of organs/ tissues and their interactions with the surgical tools. The benefits of tissue modeling are not only useful for training, planning, and practice of surgical procedures, but also optimizing surgical tool design, creating "smart" instruments capable of assessing pathology or force-limiting novice surgeons, and understanding tissue injury mechanisms and damage thresholds. Given the complexity of human organs and challenges of acquiring tissue parameters, realistic modeling and simulation of tissue mechanics is an active research area. There is a large volume of literature on the topic of tissue modeling that is distributed across the biomechanics, robotics, and computer graphics fields. For certain topics outside the scope of this review, good references are available in the literature:

- There exists a rich literature in the biomechanics community involving the measurement of tissue properties of specific organs. In the 1970s, researchers such has Fung (1973, 1993) and Yamada (1970) applied the techniques of continuum mechanics to soft tissues and conducted extensive tests to characterize tissue properties.

- Extensive work has been done by researchers in the area of computer graphics to model and simulate deformable bodies in real time (Gibson & Mirtich, 1997). The present survey does not cover work in which the focus is to produce seemingly realistic visualization effects of deformation, while ignoring the physics underlying tissue deformation.

- Approaches for complete simulator design, specific medical applications, and training evaluation methods have also been widely studied in the last two decades (A. Liu, Tendick, Cleary, & Kaufmann, 2003; Satava, 2001).

This paper summarizes the literature and presents a taxonomy (Table 1) of significant work in the field of *realistic modeling of tool-tissue interactions for simulation and robot-assisted surgery*. Since continuum mechanics provides a mathematical framework to model the deformation of biological tissues, the primary focus of this review is to compile the research done in the area of modeling and simulating surgical tool-tissue interactions in real time using the principles of continuum mechanics and finite element (FE) methods, respectively. Some other methods that could be used to simulate physically realistic tool-tissue interactions are also discussed.

This paper is organized as follows. Section 2 summarizes the basic concepts and theories of linear and nonlinear elasticity, while Section 3 provides an overview of the FE modeling technique. Sections 4 and 5 classify the prior research work that has been done in modeling non-invasive and invasive surgical tool-tissue interactions, respectively. Realistic tool-tissue interaction models requires populating models with accurate material properties and Section 6 provides a summary of some of the methods for acquiring tissue properties, and Section 7 lists some of the commercially available surgical simulators. Finally, Section 8 concludes by providing some important directions for research in the area of realistic modeling of tool-tissue interactions.

2. Continuum Mechanics for Tissue Modeling

The study of deformation or motion of a continuous material under the action of forces is known as continuum mechanics. The objective of this section is to provide a brief introduction to the mechanics of soft tissues using the theories of linear and nonlinear elasticity.

The field equations of continuum mechanics are normally formulated using tensors. An overview of tensor analysis is beyond the scope of this paper, but Ogden (1984) provides a good introduction to this subject and its application to continuum mechanics. Tensor notations and manipulations consistent with the mechanics literature are used in the derivations in this paper, e.g. bold face characters signify tensors, matrices, and vectors, while normal face characters are scalar quantities.

2.1 Kinematics of Continua

Consider a body undergoing deformation so that material points initially at $\mathbf{x}$ are mapped to spatial locations, $\mathbf{y}$. Then the deformation gradient tensor, $\mathbf{F}$, is defined by

$$\mathbf{F} = \nabla \mathbf{y}, \tag{1}$$

where ∇ is the gradient operator with respect to $\mathbf{x}$. If the displacement is $\mathbf{u}$, then $\mathbf{y} = \mathbf{x} + \mathbf{u}$. Thus,

$$\mathbf{F} = \mathbf{I} + \nabla \mathbf{u}, \tag{2}$$

where $\mathbf{I}$ is the identity tensor. A useful measure of strain is the Green strain tensor, $\mathbf{E}$, defined by

$$\mathbf{E} = \frac{1}{2}(\mathbf{F}^T \mathbf{F} - \mathbf{I}). \tag{3}$$

Substituting (2) in (3) results in

$$\mathbf{E} = \frac{1}{2}(\nabla \mathbf{u} + \nabla \mathbf{u}^T + \nabla \mathbf{u}^T \nabla \mathbf{u}). \tag{4}$$

In linear elasticity theory, strains are assumed to be small ($|\nabla \mathbf{u}| \ll 1$), hence,

$$\mathbf{E} \cong \boldsymbol{\varepsilon} = \frac{1}{2}(\nabla \mathbf{u} + \nabla \mathbf{u}^T), \tag{5}$$

where ε is the infinitesimal strain tensor. Thus, linear elasticity theory is valid only for small strains (1%–2%). One of the fundamental drawbacks of using a linear elasticity formulation to describe soft tissues is that surgically relevant strains often significantly exceed the small strain limit, invalidating the assumption of linearity. However, it is used in many simulation applications due to analytical simplicity and computational efficiency, so it is described next.

2.2 Linear Elasticity

Linear elastic modeling of soft tissues is the most widely used approach within the robotics and haptics community. Materials exhibiting linear elasticity obey the generalized Hooke's Law, which relates the stresses, $\boldsymbol{\sigma}$, and infinitesimal strains, ε, by the tensor of elastic moduli, $\mathbf{C}$, as

$$\boldsymbol{\sigma} = \mathbf{C} : \boldsymbol{\varepsilon}. \tag{6}$$

where: denotes double contraction. $\boldsymbol{\sigma}$ is also known as the Cauchy stress tensor and (6) could be rewritten as $\sigma_{ij} = \sum_{m=1}^{3} \sum_{n=1}^{3} C_{ijmn} \varepsilon_{mn}$, where C_{ijmn} is a fourth-order tensor with 81 constants, which are specific to the material. The subscript indices represent the components of the stress and strain tensor. Symmetry of the stress and strain tensors leads to $C_{ijmn} = C_{jimn}$ and $C_{ijmn} = C_{jinm}$, and the postulated existence of a strain energy density leads to $C_{ijmn} = C_{mnij}$. Thus, C_{ijmn} has 21 independent constants (called moduli) for a fully anisotropic material, i.e. a material whose properties change with direction.

If the assumption is made that the material is isotropic, then the material properties can be described by just 2 independent parameters: Young's modulus, E, and Poisson's ratio, v. E and v are related to the shear modulus, μ,

$$\mu = \frac{E}{2(1+v)}. \tag{7}$$

In the vast majority of surveyed literature (the research cited under "Linear elastic FE" in Table 1), E and v are the two parameters used to describe the soft tissue properties. Most biological materials are, however, intrinsically anisotropic. For example, a soft tissue containing fibers aligned along an axis will have different properties along and transverse to that axis. A summary of such anisotropies is presented in Spencer (1972) and Figure 2 depicts the orientation of muscle fibers in the heart (Zhukov & Barr, 2003), while the nonlinear elastic behavior of myocardial tissue and its application to surgical simulation is highlighted in Misra, Ramesh, and Okamura (2008).

2.2.1 Linear Viscoelasticity—Most soft tissues are inherently viscoelastic - they have a response based on both position and velocity. Viscoelastic materials exhibit properties of both elastic solids and viscous fluids. Similar to elastic materials, linear viscoelastic materials retain the linear relationship between stress and strain, but the effective moduli depend on time. For small strains, the general linear viscoelastic constitutive equations can be derived by separating the stresses and strains into the hydrostatic (superscript H) and deviatoric (superscript D) components:

$$\boldsymbol{\sigma} = \boldsymbol{\sigma}^{H} + \boldsymbol{\sigma}^{D} \tag{8}$$

$$\boldsymbol{\varepsilon} = \boldsymbol{\varepsilon}^{H} + \boldsymbol{\varepsilon}^{D} \tag{9}$$

Hydrostatic stresses/strains act to change the volume of the material, but maintain shape, while deviatoric or shear stresses/strains are those that distort the shape, but preserve volume (in isotropic and linear elastic materials). The hydrostatic stresses and strains are related by

$$\sigma^H = 3K\varepsilon^H, \tag{10}$$

and the bulk modulus, $K = \frac{E}{3(1-2v)}$, has small variations with time as compared to the shear modulus and hence, K considered to be independent of time. However, the deviatoric stresses and strains can be related by

$$\sum_{i=0}^{N} p_i \frac{\partial^i \sigma^D}{\partial t^i} = \sum_{j=0}^{M} q_j \frac{\partial^j \varepsilon^D}{\partial t^j}, \tag{11}$$

where p_i and q_j are material constants. In (11), the indices N and M depend on the number of material constants required to have good fit with the experimental results.

Two characteristic behaviors specific to viscoelastic materials are creep and stress relaxation. Creep occurs when a constant stress applied to the material results in increasing strain. On the other hand, stress relaxation occurs when a material is under constant strain but the stress decreases until it reaches some steady-state value. Figures 3(a) and (b) depict the behaviors of creep and stress relaxation, respectively. The one-dimensional models of creep deformation and stress relaxation are

$$\varepsilon(t) = \sigma_0 J(t) \tag{12}$$

$$\sigma(t) = \varepsilon_0 G(t), \tag{13}$$

where $J(t)$ is the "creep compliance" for constant stress, σ_0, and $G(t)$ is the "stress relaxation modulus" for constant strain, ε_0. The creep compliance and relaxation modulus are empirically determined and describe the creep and stress relaxation behavior of the viscoelastic material as a function of time.

In many cases, viscoelastic properties of soft tissues are represented by rheological models, which are obtained by connecting springs (elastic elements) and dashpots (viscous elements) in serial or parallel combinations (Fung, 1993). Three simple material models used to represent solids are the Maxwell, Kelvin-Voigt (or Voigt), and Zener standard linear solid (or Kelvin) models shown in Figures 4(a), (b), and (c), respectively.

For the Maxwell model, the relaxation behavior is acceptable, but creep behavior is insufficiently modeled. The creep compliance and stress relaxation modulus for the Maxwell model are given by

$$J(t) = \frac{1}{k} + \frac{t}{b}, \tag{14}$$

$$G(t) = ke^{\frac{-tk}{b}}.$$

(15)

where t is time. The Voigt model provides a satisfactory first-order approximation of creep, but is an inadequate model for stress relaxation. For the Voigt model, the governing equation is that of an elastic material, so there is no relaxation of stress, hence, the creep compliance is given by

$$J(t) = \frac{1}{k}\left(1 - e^{\frac{-tk}{b}}\right).$$

(16)

The Zener standard linear solid model provides a good qualitative description of both creep and stress relaxation. The creep compliance and relaxation modulus are given by

$$J(t) = \frac{1}{k_1} + \frac{1}{k_2}\left(1 - e^{\frac{-tk_2}{b}}\right),$$

(17)

$$G(t) = \frac{k_1}{k_1 + k_2}\left(k_2 + k_1 e^{\frac{-t(k_1 + k_2)}{b}}\right).$$

(18)

2.3 Nonlinear Elasticity

Elastic materials undergoing deformations with large strains (>1%–2%) are described by nonlinear elasticity theory. In order to model biological tissues, it is common to use hyperelasticity and visco-hyperelasticity (Fung, 1993). A hyperelastic material is characterized by the existence of a strain energy density function, $W(\mathbf{F})$. The stress in the material as a result of deformation can be obtained from

$$\mathbf{P} = \frac{\partial W(\mathbf{F})}{\partial \mathbf{F}},$$

(19)

where $\mathbf{P}$ is the first Piola-Kirchhoff stress tensor and $\mathbf{F}$ is the previously defined deformation gradient tensor. The Cauchy stress tensor and first Piola-Kirchhoff stress tensor are related by

$$\mathbf{P}\mathbf{F}^T = J\sigma,$$

(20)

where $J = \det(\mathbf{F})$. There are several formulations for the strain energy density function, e.g. St. Venant-Kirchhoff, Blatz-Ko, Ogden, Mooney-Rivlin, and Neo-Hookean models (Ogden, 1984). Ogden and Mooney-Rivlin strain energy density formulations provide a fairly accurately representation of the constitutive laws for many biological tissues (Holzapfel, 2000). In an Ogden model, the strain energy density function for an isotropic material is given in terms of the principal stretches, λ_i, as

$$W = \sum_{k=1}^{N} \frac{\mu_k}{\alpha_k} (\lambda_1^{\alpha_k} + \lambda_2^{\alpha_k} + \lambda_3^{\alpha_k} - 3),$$

(21)

where $\lambda_1 \lambda_2 \lambda_3 = 1$, i.e. thermal incompressibility, and μ_k and α_k are material parameters determined from experiments. The Mooney-Rivlin model commonly used to represent rubber-like materials, is widely used for soft tissues and is given in terms of the principal invariants, I_i, for isotropic and incompressible materials as

$$W = C_1(I_1 - 3) + C_2(I_2 - 3),$$

(22)

where C_1 and C_2 are material constants. The principal invariants are defined in terms of right Cauchy-Green tensor, $\mathbf{C} = \mathbf{F}^T \mathbf{F}$, as

$$I_1 = \mathbf{C}:\mathbf{I},$$

(23)

$$I_2 = \frac{1}{2} \left((\mathbf{C}:\mathbf{I})^2 - (\mathbf{C}:\mathbf{C}) \right),$$

(24)

$$I_3 = \det \mathbf{C}.$$

(25)

Some researchers have used the Neo-Hookean model to represent soft tissues. The Neo-Hookean strain energy density function is a special case of the Mooney-Rivlin model and is given by

$$W = C_1(I_1 - 3).$$

(26)

If material parameter constants for Ogden or Mooney-Rivlin models are defined in terms of creep and stress relaxation functions, then the material can be modeled as visco-hyperelastic, which may represent the realistic behavior of many soft tissues (Fung, 1993).

3. Finite Element Modeling

The FE method is a numerical technique for solving field equations, typically partial differential equations, and has been used in the last decade to simulate soft tissue deformation by solving the equations of continuum mechanics. The FE method originated from the need to find approximate solutions to complex problems in elasticity and vibration analysis (Cook, Malkus, & Plesha, 1989). Its development can be traced back to the work by Hrennikoff (1941) and Courant (1942) (Fung & Tong, 2001). Over the years, the FE method has spread to applications in many different areas of engineering, including structural analysis in civil and aeronautical engineering, thermal analysis, and biomechanics. Numerous FE computer programs are commercially available for general or specific applications. These include ABAQUS (Simulia), ADINA (ADINA R & D Inc.), ANSYS (ANSYS Inc.), DYNA3D (Lawrence Livermore National Laboratory), FEMLAB (COMSOL Inc.), GT STRUDL (Georgia Tech-

CASE Center), NX I-deas (Siemens PLM Software), and NASTRAN (MSC Software Corp.). This section provides a very high-level overview of the FE method; there are numerous textbooks that deal with this subject, e.g. Cook et al. (1989), Desai and Abel (1972), and Zienkiewicz, Taylor, and Zhu (2005).

In the FE method, the continuum is divided or meshed into a finite number of sub-regions called *elements*, such as tetrahedrons, quadrilaterals, etc. Two adjacent elements are connected via *nodes*. The elastic behavior of each element is categorized using matrices in terms of the element's material and geometric properties, and distribution of loading within the element and at the nodes of the element. Linear or quadratic *shape* or *interpolation functions* are used to approximate the behavior of the field variables at the node. The element behavior is characterized by partial differential equations governing the motion of material points of a continuum, resulting in the following discrete system of differential equations:

$$\mathbf{M\ddot{u}+C\,\dot{u}+Ku=F-R},$$

(27)

where $\mathbf{M}$, $\mathbf{C}$, and $\mathbf{K}$ are the element mass, damping, and stiffness matrices, respectively. $\mathbf{u}$ is the vector of nodal displacements, and $\mathbf{F}$ and $\mathbf{R}$ are the external and internal node force vectors, respectively. All these matrices and vectors may be time dependent. One approach to solve (27) in a quasi-static manner is by setting $\mathbf{\ddot{u}} = \mathbf{\dot{u}} = 0$. Thus, with every simulation iteration, a large number of element-stiffness and element-force vectors are assembled, which leads to a system of algebraic equations, called the global system. The accuracy and numerical efficiency of the FE method lies largely in the development of effective pre- and post-processors, and algorithms for efficiently solving large systems of equations. On the other hand, (27) can be solved with a dynamic approach, using implicit or explicit integration schemes. For explicit integration methods, the state at a given instant is a function of the previous time instants, while for the implicit scheme, the state at a certain instant cannot be explicitly expressed as a function of the state at the previous time step. The implicit scheme involves inversion of the stiffness matrix at each time step, typically a computationally expensive process. The explicit scheme can be easily implemented by avoiding the matrix inversion process but suffers from numerical instability under inappropriately chosen integration time step. Thus, the explicit time integration is only conditionally stable, potentially requiring very small time steps to provide a suitably accurate and stable solution. Properly designed implicit methods, can be numerically stable over a wide range of integration time step values. Hence, they are preferable for simulation of systems described with stiff and nonlinear differential equations.

In recent years, FE methods have been applied to simulate the responses of tissues and organs. Biological tissues are anisotropic, inhomogeneous, undergo large strains, and have nonlinear constitutive laws, and FE techniques presents an attractive method to numerically solve such complex problems. However, most commercial FE codes are optimized for linear elastic problems. The number of nonlinear elastic material models available in most codes is quite limited and are sensitive to small variations in material properties. There also exist numerous challenges for realistic simulation of organs and their application to surgical simulators. In general, the finer the mesh in an FE model, the more accurate the simulation. But a greater number of elements leads to more computational time, which hampers the ability of the simulator to run in real time. The speed of the simulation may depend on the constitutive law used, the material parameters chosen, and the scale of the deformation. Further, it is difficult to obtain the material properties of an inhomogeneous and anisotropic organ, which limits the accuracy of results obtained from an FE model. Also, organs have anatomically complex geometries and boundary conditions, which are difficult to model. Despite these limitations and challenges, the FE technique remains the most widely used numerical method for realistic modeling of surgical tool-tissue interactions.

4. Non-Invasive Soft Tissue Deformation Modeling

Having described the fundamental mechanics and simulation techniques required for realistic soft tissue modeling, we now begin the literature survey. We classify surgical tasks that do not involve tissue rupture as non-invasive tasks. Several modeling methods have been considered in the literature for modeling local and global tool-tissue interactions. Some studies have also investigated the effect of the tool geometry on interaction forces. Figures 6(a), (b), (c), and (d) provide some examples of the tools used to measure tool-material interaction forces (Mahvash, Hayward, & Lloyd, 2002). It was observed that changes in tool geometry caused variations in the force-deflection responses only for large localized deformations of the material.

Most of the research presented in this section considered either distributed uniaxial compressive loads or loads exerted by indentors, without focusing on the tool geometry. For the purpose of building models for surgical simulators, this section categorizes the various non-invasive tissue modeling techniques as linear elasticity-based and nonlinear (hyperelastic) elasticity-based FE methods, and other methods which do not fall into the realm of continuum mechanics and/or do not use FE methods for simulation.

4.1 Linear Elastic Finite Element Models

Linear elasticity-based FE models are probably the most widely used techniques to model tissue deformation in surgical simulators. Motivating factors are simplicity of implementation and computational efficiency, which enables real-time haptic rendering, since only two material constants are needed to describe isotropic and homogenous materials, as stated in (7). This section describes the modeling of tool-tissue interactions using linear elasticity-based FE methods.

In general, due to the steps involved in setting-up and running a FE calculation, linear or nonlinear elasticity-based FE models cannot be simulated in real time. Hence, some researchers have focused efforts on optimizing FE-based computational techniques to be applicable to surgical simulators. Bro-Nielsen (1998) was one of the first researchers to apply the condensation method to a FE model for real-time surgical simulations. This method is based on the idea that only displacement of nodes that are in the vicinity of the tool need to be rendered. It was shown that nodal displacements resulting from this method are similar to those obtained from conventional linear FE analysis. Comparison studies were performed on a FE model of the human leg having 700 system nodes. Tensile and compressive loads were applied to 3 nodes on the calf area of the leg while one edge of the leg was fixed. Cotin, Delingette, and Ayache (1999) created real-time heptatic surgery simulations using a modified FE method wherein the bulk of the computations were performed during the pre-processing stage of the FE calculation. Using data from computed tomography (CT) scans, they also built a three-dimensional anatomical model of the liver and used linear elasticity-based modeling to simulate its deformation. Basdogan, Ho, and Srinivasan (2001) and Kühnapfel, Çakmak, and Maaß (2000), used linear elastic theory for developing simulators for laparoscopic cholecystectomy (gallbladder removal) and endoscopic surgical training, respectively. In order to enable real-time visual and haptic simulation, Basdogan et al. (2001) only considered the significant vibration modes to compute tissue deformation, while Kühnapfel et al. (2000) implemented the previously mentioned condensation method. An example of a non-real-time surgical simulation system using linear FE modeling is that of Gladilin, Zachow, Deuflhard, and Hege (2001), who used a conventional linear FE model to simulate tissue deformations for craniofacial surgery. Their simulation does not run in real time.

The models discussed above typically used assumed material properties, and were not validated by comparing them with experimental results. Some researchers, however, have attempted to develop their linear elastic FE models based on experimental studies conducted on phantom

or real tissue. Since non-invasive tool-tissue interaction modeling is a subset of the invasive surgical procedures, researchers such as DiMaio and Salcudean (2003a), and a few others presented in Table 1 (under invasive surgical procedures) first performed indentation or other non-invasive measurements to characterize the tissue properties. Gosline, Salcudean, and Yan (2004) developed a FE simulation model and coupled it to the haptic device used by DiMaio and Salcudean (2002). In Gosline et al. (2004), the authors used a linear elasticity-based FE model to simulate organs filled with fluid. Simulations were compared with experimental studies done on phantom tissue with a fluid pocket. The phantom tissue was deformed with a known load, while the fluid pocket was imaged using ultrasound and the surface of the tissue was tracked using a digitizing pen. Kerdok et al. (2003) devised a method to measure the accuracy of soft tissue models, by comparing experimental studies against FE models. They built the "Truth Cube" (Figure 7(a)), which was a silicone cube embedded with fiducials having Young's modulus of 15 kPa. They found good agreement between the experimental and simulation results for small strains (1%–2%), where linear elasticity theory is valid. As expected, the linear elasticity-based FE method did not compare well against the experimental results for large strains. Figure 7(b) depicts the CT image for large strain indentation case. The results from the imaging studies were compared to the FE model, shown in Figure 7(c). Sedef, Samur, and Basdogan (2006) used a linear viscoelastic model where the material properties, time constants for the relaxation function, and normalized values of shear moduli were derived from indentation experiments performed *in vivo* on porcine liver.

4.2 Hyperelastic Finite Element Models

Soft tissues undergo large deformations during surgical procedures and the study of nonlinear solid mechanics, specifically hyperelasticity, provides a framework for analyzing such problems. The key to studying large deformation problems is the identification of an appropriate strain energy function. Once the strain energy function is known, the constitutive stress-strain relationships can be derived. A vast majority of the strain energy functions used for biological soft tissues are adapted from those used to model polymers and rubber-like materials. The Arruda-Boyce model (Arruda & Boyce, 1993), which is based on statistical mechanics and normally used to model rubber, has been used to simulate palpation of breast tissues in Y. Liu, Kerdok, and Howe (2004). X. Wu, Downes, Goktekin, and Tendick (2001) implemented the widely used Mooney-Rivlin model to simulate tissue deformation in the training simulator developed by Tendick et al. (2000). They introduced the concept of dynamic progressive meshing to enable real-time computation of deformation.

In order to develop the best possible constitutive model and add greater realism to the tissue model, several researchers have used experimental data and elaborate setups to populate the coefficients of the strain energy function. Carter, Frank, Davies, McLean, and Cuschieri (2001) conducted several indentation tests on sheep and pig liver, pig spleen *ex vivo*, and human liver *in vivo* for the intended development of a laparoscopic surgical simulator. An exponential relationship that relates the stress to the stretch ratio, developed by Fung (1973), was used to fit the experimental data. Davies, Carter, and Cuschieri (2002) conducted large and small probe indentation experiments on unperfused and perfused pig spleen for potential use in surgical simulators. The experimental data were fitted with a hyperelastic model of Neo-Hookean, Mooney-Rivlin, and exponential forms. The goal of their study was to underscore the fact that experimental studies are required to build realistic tool-tissue interaction models, and the hyperelastic model of exponential form is suitable for modeling pig spleen. Hu and Desai (2004) and Chui, Kobayashi, Chen, Hisada, and Sakuma (2004) based their model on results obtained from pig liver. In Hu and Desai (2004), the authors compared results obtained from Mooney-Rivlin and Ogden models, while Chui et al. (2004) considered several strain energy functions that were combinations of polynomial, exponential, and logarithmic forms. Chui et al. (2004) concluded that both the Mooney-Rivlin model with nine material constants and the

combined strain energy of polynomial and logarithmic form with three material constants were able to fit the experimental data. The lowest root mean square error of 29.78 ± 17.67 Pa was observed between analytical and experimental results for the tension experiments where the maximum stresses were in the order of 3.5 kPa. Molinari, Fato, Leo, Riccardo, and Beltrame (2005) present a model of the scalp skin to be used by plastic surgeons for pre-operative planning. The authors assumed a strain energy function of polynomial form with four parameters dependent on the skin tissue. The maximum nodal displacement between the simulated and experimental results was observed to be 0.45 mm for load cases ranging from 5 N to 50 N.

4.3 Visco-Hyperelastic Finite Element Models

Real soft tissues exhibit both viscoelastic and nonlinear properties. Thus, the coupling of viscoelastic and hyperelastic modeling techniques results in a more realistic representation of soft tissues. Puso and Weiss (1998) were the first to implement an anisotropic visco-hyperelastic FE model for soft tissue simulations and applied this technique to model the femur-medial collateral ligament-tibia complex. In order to model the quasi-linear viscoelastic behavior, the authors used an exponential relaxation function. This was coupled with the Mooney-Rivlin model to represent hyperelasticity of the tissue. Though simulation data were not compared with real tissue data and this work does not represent a surgical tool-tissue interaction model, it provides an elegant FE modeling framework for modeling soft tissues.

The endoscopic surgical simulator developed at ETH is one of the few complete systems that incorporates continuum mechanics-based tool-tissue interaction modeling techniques, and provides realistic visualization and haptic feedback in real time (Székely et al., 2000). The simulator development at ETH is the culmination of many years of work and taps into the expertise of several engineering disciplines (Hutter, Schmitt, & Niederer, 2000; Székely et al., 2000; Vuskovic, Kauer, Székely, & Reidy, 2000). They built a very detailed anatomical model of the uterus to be simulated, followed by the development of a three-dimensional homogenous isotropic FE model of the organ and populated it with real tissue material properties. Further, they designed parallel computing capability for the simulator to function in real time and integrated a custom-built force feedback device that would enable simulation of hysteroscopy. The authors used a novel tissue aspiration method to capture the force-displacement relationship of the uterine tissue *in vivo*. A hyperelastic model (Székely et al., 2000) with five material constants and visco-hyperelastic model (Vuskovic et al., 2000) with two material constants and two constants due to the stress relaxation function, were considered by the authors. Nava, Mazza, Haefner, and Bajka (2004) used the tissue aspiration method of Vuskovic et al. (2000) on bovine liver and focused on modeling the preconditioning phase of soft tissue. The authors believe that characterizing this phenomena can provide information on the capabilities of the tissue to adapt to load and recover to its original configuration when unloaded during surgical tool and tissue interactions. A reduced polynomial form of the strain energy function was used to model hyperelasticity. Thirteen material constants relating to the visco-hyperelastic model were deemed sufficient to match the experimental data. Figures 8(a) and (b) depict the FE model and tool-tissue interaction presented in Székely et al. (2000), respectively.

A few other researchers have also used visco-hyperelastic models to simulate soft tissue behavior, though their studies are not as detailed as the work presented in Székely et al. (2000). Work in accurate fitting of hyper-viscoelastic constitutive models to real tissue data is presented below. Kim, Tay, Stylopoulos, Rattner, and Srinivasan (2003) and Kim and Srinivasan (2005) used data from indentation experiments on porcine esophagus, liver, and kidney. They fit a Blatz-form strain energy function to force-displacement data obtained from quasi-static experiments, while both linear (Kelvin) and nonlinear viscoelastic models were

used to fit force-time data from dynamic experiments (Kim et al., 2003). A Mooney-Rivlin model was used in Kim and Srinivasan (2005). The nonlinear viscoelastic model consisted of several springs in parallel with nonlinear stiffness and was able to match the stress relaxation curves derived from dynamic experiments. Miller (2000) and Miller and Chinzei (2002) presented a visco-hyperelastic model to simulate the tissue response of pig brain to external loads. In Miller (2000), biphasic (tissue is assumed to be a mixture of a solid deformable porous matrix and a penetrating fluid) and single phase models were evaluated, and the single phase model showed good correlation with the experimental data for up to ~30% strains. The visco-hyperelastic models considered were in terms of strain invariants and fractional powers of principal stretches in Miller (2000) and Miller and Chinzei (2002), respectively. Both models had two independent material parameters and one parameter relating to the stress relaxation function. In Miller (2000), theoretical results were also compared with published *in vivo* stress-strain data for Rhesus monkey liver and kidney. Real-time implementation of the simulation models has not been shown.

4.4 Other Modeling Methods

The primary motivation for choosing a tissue modeling technique that is not based on linear elasticity or hyperelasticity-based FE methods is to generate a computationally efficient simulation model. These specialized models are designed for straightforward implementation and could be used for static and dynamic computation, as described in Section 3. The realism of tissue deformation can be compromised as a result of such modeling simplicities since it is difficult to relate fundamental tissue properties to these models.

Mass-spring-damper models are the most common non-continuum mechanics-based technique used for modeling soft tissues. Organs have been modeled by combining the spring-damper models, described in Section 2.2.1, in series or parallel combination. In this case, a set of points are linked by springs and dampers, and the masses are lumped at the nodal points. Delingette, Subsol, Cotin, and Pignon (1994), Keeve, Girod, and Girod (1996), Koch et al. (1996), Castañeda and Cosío (2003), and Waters (1992) are some of the studies that have used mass-spring-damper models to simulate tissue deformation, but they do not provide any information on the tissue properties required for the simulation. On the other hand, d'Aulignac, Balaniuk, and Laugier (2000) used a sophisticated apparatus for data acquisition to enable virtual ultrasound display of the human thigh while providing force feedback to the user. The model for the human thigh was composed of a mass-spring system whose physical parameters were based on an earlier study conducted by authors (d'Aulignac, Laugier, & Cavusoglu, 1999). The two layer model was composed of a mesh of masses and linear springs, and set of nonlinear springs orthogonal to the surface mesh to model volumetric effects. The novelty of this research was that in order to provide real-time haptic feedback to the user, the authors have incorporated a buffer model between the physical model and haptic device. This computationally simple model locally simulates the physical model and can estimate contact forces at haptic update rates. The buffer model was defined by a set of parameters and was continuously adapted in order to fit the values provided by the physical model.

In addition to continuum mechanics and FE methods, other innovative approaches have been developed to achieve real-time performance. In order to ease the computation burden caused by using FE-based modeling techniques, without resorting to non-physical methods such as mass-spring-damper models, researchers have tried to implement models with two-dimensional distributed elements filled with an incompressible fluid. Such models are known as the Long Element Models (LEM) and the advantage of this method is that the number of the elements is one order of magnitude less than in a FE method based on tetrahedral or cubic elements. Balaniuk and Salisbury (2002) presented the concept of LEM to simulate deformable bodies. Their approach implements a static solution for linear elastic global deformation of

objects based on Pascal's principle and volume conservation. Using this method, it is possible to incorporate physically-based simulation of complex deformable bodes, multi-modal interactivity, stable haptic interface, changes in topology, and increased graphic rendering, all done in real time. The use of static equations instead of partial differential equations avoids problems concerning numerical integration, ensuring stability during simulation. Sundaraj, Mendoza, and Laugier (2002) used the concept of LEM to simulate palpation of the human thigh with a probe, where the average linear elastic material constant was derived from experimental studies. Sagar, Bullivant, Mallinson, Hunter, and Hunter (1994) presented a detailed and complete training system for ophthalmological applications. Their micro-surgical training system included a teleoperated device for the user to interact with the virtual model eye, a high-fidelity three-dimensional anatomical model of the eye, and a FE model of the cornea. Modeling of the collagen fibers in the cornea was done using nonlinear elastic J-shaped uniaxial constitutive laws. Simulation tests concluded that the virtual environment was able to provide graphics in real time. Similar to all the studies mentioned in this section, no comparisons have been made between simulation results and actual tissue deformations during micro-surgery in the eye. In essence, Sagar et al. (1994) used a FE technique for simulation, but the soft tissues were not modeled using linear or hyperelastic models, and hence this work is classified in this section.

FE modeling methods can be extremely sensitive to mesh resolution, hence in the last decade studies have been done to avoid using meshes altogether. Such meshless, particle, or finite point methods share the characteristic that there is no need to explicitly provide the connectivity information between the nodes. De, Kim, Lim, and Srinivasan (2005) described a meshless technique for modeling tool-tissue interactions during minimally invasive surgery. They call this method the Point Collocation-based Method of Finite Spheres (PCMFS), wherein computational particles are scattered on a domain which are linked to a node. Approximation functions are defined on each particle and are used to solve the differential equations based on linear elasticity. The PCFMS proved to be computationally superior than commercially available FE packages, and performed simulations in real time. The authors are currently extending PCFMS to include nonlinear elastic properties of tissues and future work would enable users to simulate tissue cutting. The work presented in De et al. (2005) is based on continuum mechanics but does not use FE techniques for simulation; hence, it is grouped in this section. In De, Lim, Manivannan, and Srinivasan (2006), the authors extended the concept of PCMFS to Point-Associated Finite Field Approach (PAFF), where points are used as computational primitives and are connected by elastic force fields. PAFF also assumes linear elasticity for modeling soft tissues. De and Srinivasan (1999) presented an innovative method to model soft tissue by modeling organs as thin-walled membranes structures filled with fluid. Using this technique, it was possible to model experimental data obtained *in vivo*, though the authors did not provide information on the simulation input parameters.

In order to add realism to their simulation models, some researchers have performed experimental studies to populate their models with material parameters. Hu and Desai (2003) described a hybrid viscoelastic model to fit the experimental results obtained during indentation experiments on pig liver. The hybrid model uses linear and quadratic expressions to relate the measured force-displacement values, which are valid for small strains (up to 16% compression) and large strains (from 16% – 50% compression), respectively. The model used by the authors represents the local surface deformation of liver. James and Pai (2001) have achieved real-time interaction by using boundary element models. If the geometry, homogeneous material properties, and boundary conditions of the model are known, then reasonable graphical update rates are achievable by precomputing the discrete Green's functions of the boundary value problem. A force interpolation scheme was used to approximate forces in between time steps which allowed for higher haptic update rate than the visual update rate. Inhomogeneous materials cannot be supported by the boundary element

analysis technique, which is a disadvantage in applications for surgical simulation. Lang, Pai, and Woodham (2002) used to the concept of Green's functions matrix for linear elastic deformation. The estimation of the Green's function matrix was based on local deformations while probing an anatomical soft-wrist model and plush toy. The global deformations were based on the range-flow on the object's surface. Simulation and experimental results have not been compared.

5. Invasive Soft Tissue Deformation Modeling

Almost all surgical procedures involve tissue rupture and damage, either by cutting using scissors, a blade, or procedures such as electro-cautery, or during operations involving needle insertion. Hence, realistic modeling and simulation of these two operations is probably the most important requirement for a surgical simulator. Further, complex but common procedures like suturing could be extrapolated from the techniques developed for modeling cutting and needle insertion. Modeling and simulation of invasive procedures involves constantly changing boundary constraints and accurate modeling of friction, which are difficult to measure. Accurate models of friction become especially important when simulating minimally invasive surgical procedures, in which the surgeon has no direct contact with the tissue, but manipulates the tissue via laparoscopic instruments. In this case, not only must sliding friction between the instruments and the organs be accounted for, but friction in the trocar and hinges must be modeled. Organs are connected to bones, muscles, and/or other organs via connective tissue. Hence, modeling of these connective tissues is also essential to simulate accurate response of the organ for both non-invasive and invasive procedures. Similar to modeling of non-invasive surgical procedures, linear elasticity-based FE models have been the most prevalent technique for simulating invasive operations. Very few studies have invoked nonlinear elasticity-based FE methods. Some modeling techniques that are not based on continuum mechanics are also described in this section.

5.1 Finite Element Methods

As mentioned earlier, the ability to model the response of soft tissue during needle insertion and/or cutting is of primary importance in the development of realistic surgical simulators. Modeling and simulation of invasive tissue deformation in a FE framework is significantly more challenging than non-invasive modeling primarily due to two factors. First, it is difficult to measure the fracture toughness of inhomogeneous soft tissues to accurately model the rupture process. Second, invasive surgical simulation involves breaking and remeshing of nodes, which is computationally expensive for reliable simulation. Nonetheless, simulation of needle insertion through soft tissue is an active research area because of applications in minimally invasive percutaneous procedures like biopsies and brachytherapy. Research in needle insertion has examined the following topics: modeling and simulation of needle-tissue interaction forces, tissue deformation, deflection of the needle during insertion, path-planning of needle trajectories based on tissue deformation, and devising experimental setups for robot-assisted needle insertion. Also, modeling of surgical cutting has focused on using single blade scalpels or surgical scissors to model the resulting soft tissue deformation. In this section we focus on recent studies of modeling tool-tissue interaction forces and tissue response during invasive procedures using FE methods, while in Section 5.2 we highlight methods not based on continuum mechanics.

5.1.1 Linear Elastic Simulations—Tissue and needle interactions have been studied by the robotics community primarily for path planning of surgical procedures. DiMaio and Salcudean (2005) were the first to develop an interactive linear elastic FE simulation model for needle insertions in a planar environment. The simulated needle forces matched experimental data using a phantom tissue of known material properties and achieved real-time

haptic refresh rates by using the condensation technique (Bro-Nielsen, 1998) during pre-processing. Tissue modeling techniques have also been implemented in steering of needles by Alterovitz, Goldberg, Pouliot, Taschereau, and Hsu (2003) and DiMaio and Salcudean (2003b). Further, Goksel, Salcudean, DiMaio, Rohling, and Morris (2005) extended the work done by DiMaio and Salcudean (2003a) to integrate needle insertion simulations in three-dimensional models. Figures 9(a), (b), and (c), depict the experimental and simulation work done in DiMaio and Salcudean (2003a).

A two-dimensional linear FE model for needle insertion during prostate brachytherapy is presented in Alterovitz et al. (2003). This study fine-tuned the simulation parameters to prostate deformation results obtained from a surgical procedure, but did not independently compare their model to data obtained by needle insertion with real or phantom tissues. Their results indicate that seed placement error depends on parameters such as needle friction, sharpness, and velocity, rather than patient specific parameters (tissue stiffness and compressibility). Crouch, Schneider, Wainer, and Okamura (2005) used experiments and FE modeling to show that a linear elastic tissue model in conjunction with a dynamic force function could accurately model interaction forces and tissue deformation during needle insertion. They used a phantom tissue model with known material properties and concluded that the accuracy of the model diminished during the relaxation phase, because soft tissue is viscoelastic. Hing, Brooks, and Desai (2006) captured the different phases of interaction between needle and pig liver. Using experimental data, the authors estimated the linear effective modulus of the tissue sample during puncture at various speeds.

Cutting is the most common invasive surgical procedure, and this operation has been modeled by some researchers using linear elastic FE models (Picinbono, Lombardo, Delingette, & Ayache, 2000; W. Wu & Heng, 2005). Picinbono et al. (2000) discussed the software for a prototype laparoscopic surgical simulator which used linear extrapolation over time and position of the interaction forces to render haptic feedback to the user. W. Wu and Heng (2005) presented a hybrid condensed FE model, which consisted of operational and non-operational regions. The authors assumed that topological changes only occur in the operational part. The algorithm proved to be computationally efficient, but for both studies (Picinbono et al., 2000; W. Wu & Heng, 2005), no comparison between simulated and experimental results were presented. Chanthasopeephan, Desai, and Lau (2003) computed the local effective Young's modulus of pig liver during cutting experiments. Different values of the effective modulus were obtained for plane strain, plane stress, and quasi-static models, and there was a decrease in liver resistance as the cutting speed increased.

5.1.2 Hyperelastic Simulations—Due to the computational burden of using FE methods for modeling invasive surgical procedures coupled with the difficulty in characterizing the nonlinear behavior of real tissues during rupture, very few studies have implemented hyperelastic models. Nienhuys and van der Stappen (2004) used a compressible Neo-Hookean material model for simulating needle insertion in a three-dimensional organ model. The study was purely based on simulations and no comparisons between real and simulation data were provided. To date, only one study by Picinbono, Delingette, and Ayache (2003) has implemented a nonlinear anisotropic model to simulate cutting of liver (hepatic resection). The anisotropic framework is similar to the study done in Picinbono et al. (2000), and this work was extended to include hyperelasticty based on the St. Venant-Kirchhoff model. Figure 10(a) depicts the difference in deformation between the linear and nonlinear elasticity-based models, while Figure 10(b) provides a screenshot simulating electro-cautery of the liver. No validation or comparison of the simulation model was presented.

5.2 Other Methods

As discussed earlier, modeling and simulation of invasive procedures requires modification of organ topology with time. Using FE methods is generally computationally expensive, hence, several studies have looked at alternative modeling methods. These are presented in this section. The objective of Glozman and Shoham (2004) was to formulate path planning algorithms for flexible needles. Virtual springs were placed orthogonal to the needle insertion axis in order to model the needle-tissue interaction force. They did not mention the stiffness of the springs used in the simulations, but the authors claim they can be determined experimentally or from pre-operative images. In order to compute soft tissue deformations while simulating prostate brachytherapy, Wang and Fenster (2004) used a restricted three-dimensional ChainMail method. In the ChainMail formulation, each volume element is linked to its six nearest neighboring elements in the front, back, top, bottom, left, and right. When any of the elements is displaced beyond its defined limit (constraint zone), the neighboring element absorbs the movement due to the flexibility of the structure. The authors proposed a restricted ChainMail method by constraining the angular component of the shear constraint. The three-dimensional prostate image was segmented based on the restricted ChainMail method. Since soft tissue deformation was not based on actual deflection data of the prostate, although the simulations could be performed in real time and were visually pleasing, one cannot be certain of the realism in tissue deformation. Kyung, Kwon, Kwon, Kang, and Ra (2001) developed a simulator for spine needle biopsy using the voxel-based haptic rendering scheme. A three-dimensional human anatomical model was generated by segmenting images derived from CT scans or magnetic resonance imaging (MRI). The organs modeled in the region of the lumbar vertebra were bones, lung, esophagus, arteries, skin, muscle, kidney, fat, and veins. The soft tissues were modeled as a series of springs, which is not realistic. The spring stiffness was determined using needle force and insertion depth obtained from experimental results in a previously conducted study (Popa & Singh, 1998). The skin deformation and puncture forces were modeled as a nonlinear viscoelatic model. The simulated forces were calculated from interactions between volume image data and the pose of the needle.

In addition to developing efficient algorithms to simulate tissue rupture, the researchers presented below also conducted experimental studies to populate their models with realistic tissue data. Brett, Parker, Harrison, Thomas, and Carr (1997) described the design of a surgical needle resistance force simulator for the purpose of training and improving skills required for epidural procedures. The tissue model was composed of a Voigt mass-spring-damper model. The skin, muscular and ligmental tissues, connective tissue and fascia, and fat were modeled as nonlinear viscoelatic solid, elastic membrane, and viscous solid, respectively. The material parameters were based by fine tuning the results obtained from porcine samples and cadavers. A similar modeling technique was used by Brett, Harrison, and Thomas (2000), in combination with an elaborate laser-based spectroscopy technique for determining tissue type and measuring tissue deformation. Brouwer et al. (2001) fitted an exponential relationship between the applied force and the stretch ratio, which were derived from experimental data on various porcine abdominal organs. Measurements were performed both *in vivo* and *ex vivo* during needle insertion and cutting tasks in order to develop a web database of tool-tissue interaction models. The objective of the work done by Okamura, Simone, and O'Leary (2004) was to model the forces during needle insertion into soft tissue. Experimental studies were conducted *ex vivo* on bovine liver, with intended applications for liver biopsy or ablation. They divided the forces during needle insertion into forces during initial puncture, due to friction, and during cutting. The forces during initial puncture were modeled as a nonlinear spring. The spring constants were obtained by curve fitting the experimental data and wide variation in data was observed for these constants. A Karnopp friction model which includes both the static and dynamic friction coefficients was used to model the friction during needle insertion. Finally,

the cutting forces were obtained by subtracting the puncture and friction force from the total measured force.

A clever modeling technique would incorporate realistic tool-tissue interactions from FE models and computational efficiency from mass-spring models. Such a hybrid model was presented by Cotin, Delingette, and Ayache (2000) to simulate soft tissue deformation and cutting. The quasi-static linear elastic FE model introduced by the authors was computationally efficient but did not allow topological changes to the model. On the other hand, the mass-spring model could simulate tearing and cutting in real time, but was not visually appealing. So the authors combined the above models, such that the small region of tool-tissue interaction was composed of a mass-spring model, while the major part of the organ underwent deformation based on the linear elastic FE model. Simulation results showed that this hybrid method was computationally efficient. However it is very difficult to relate mass-spring parameters to actual material parameters.

All the previously mentioned models in this section have focused on global deformation of tissue while interacting with a surgical tool, while the local tool-tissue interaction is simulated as a remeshing problem ignoring the energetics of cutting. In the studies presented below, the researchers investigated and modeled local tissue damage. Mahvash and Hayward (2001) attempted to model cutting of soft tissues using the fracture mechanics approach. They modeled cutting of soft tissues as an elastic fracture undergoing plastic deformation near the crack, but soft tissues in general are not linear elastic. The process of cutting was divided into three subtasks: deformation, cutting, and rupture, where energy exchange occurs. In the formulation, Mahvash and Hayward (2001) used fracture toughness to describe the material property. Experimental tests were conducted on potato sample and bovine liver. In order to match experimental results with software simulation results, the authors tweaked the material parameters to get the best match. Further, for the experimental studies on liver, the authors were unable to predict the different phases of fracture. Okamura, Webster III, Nolin, Johnson, and Jafry (2003) presented the "Haptic Scissors", a two-degree of freedom device that provides the sensation of cutting in virtual environments by providing force feedback. In this study, they discussed an analytical framework to model tissue cutting, and showed via experimental studies that the users could not differentiate between the analytical model and haptic recordings created earlier. The analytical model was a combination of friction, assumed material properties, and user motion to determine cutting forces. This simplified model did not take into account the material variations in biological tissues. The forces felt by the user at the handle were assumed to be a summation of forces from friction at the scissor pivot and scissor blades, and the cutting force. The data from the analytical model did not match experimental data because the user grip force, inhomogeneous tissue properties, and elastic forces in the tissue, were not modeled. Mahvash and Okamura (2005) and Mahvash, Voo, Kim, Jeung, and Okamura (2007) applied the framework developed in Mahvash and Hayward (2001) to the "Haptic Scissors". A physically valid model would have a hyperelastic model describing the global tissue response while interacting with the tool and the local response would be governed by fracture mechanics.

6. Methods for Model Acquisition

The importance of having accurate tissue models has been recognized as a key requirement for realistic and practical surgical simulators. This section presents of some of the current experimental techniques for extracting tissue properties both *in vivo* and *ex vivo*, and using invasive and non-invasive methods. Broadly, there exist two approaches to acquire tissue properties for building surgical simulators: global and local measurement. The choice of measurement is dictated by the intended surgical simulation procedure and in turn results in the type of experimental setup developed. The design of the apparatus used is based on the

organ's structure and composition, boundary conditions, and how the organ is to be loaded in order to extract force-displacement readings.

The most prevalent form of measuring local material properties of tissues involves indentation, uniaxial compression/tensile, and/or shear experiments performed *ex vivo* on a tissue sample. The applied force and tissue displacement are recorded and a constitutive law or force-displacement relation that best fits the experimental results is determined. Most of this research uses phantom or *ex vivo* tissues, although *in vivo* tissues may have significantly different dynamics due to variations in temperature, surrounding and internal blood circulation, and complex boundary constraints, which are almost impossible to replicate during *ex vivo* testing. Hence, some researchers have used elaborate schemes to perfuse the organ *ex vivo*, so as to not compromise the inherent tissue properties that are observed *in vivo* (Ottensmeyer, Kerdok, Howe, & Dawson, 2004). On the other hand, some researchers have developed novel devices to measure tissue properties *in vivo* (Brown, Rosen, Sinanan, & Hannaford, 2003; Vuskovic et al., 2000). Brown et al. (2003) presented the "modified surgical graspers", while Vuskovic et al. (2000) proposed the "tissue aspiration technique", as shown in Figure 11(a). Brouwer et al. (2001) described instrumentation to measure the soft tissue-tool forces and tissue deflection, both *in vivo* and *ex vivo*. The following tests were performed in a pig's abdominal cavity: grasping the pig intestine wall in the longitudinal and transverse directions, indentation, needle insertion during suturing, and cutting using scissors. Further, Ottensmeyer (2002) described the TeMPeST 1-D (1-axis Tissue Material Property Sampling Tool), as shown in Figure 11 (b), which can be used to measure linear viscoelastic properties of soft tissue *in vivo*. TeMPeST 1-D is inserted laproscopically into the pig, and a waveform is commanded to the instrument. Data sampling takes approximately 20 seconds. Such localized measurement of tissue properties only provides information about a specific region of the organ, and for the purposes of modeling, local properties are usually assumed to describe the behavior of the complete organ. But as mentioned earlier, human organs are anisotropic and inhomogeneous, and in some cases tissue properties vary significantly from one location to another for the same organ. Further, with localized measurement and modeling techniques, it is not possible to account for the organ geometry and complex boundary conditions.

In light of the shortcomings mentioned above, some researchers have focused on assessing the global deformation of tissues to applied loads. These techniques have typically involved placing fiducial markers on the top of the tissue sample (DiMaio & Salcudean, 2003a) or embedding markers (Crouch et al., 2005; Hing et al., 2006; Kerdok et al., 2003) within the tissue sample. As shown in Figures 9(a) and (b), DiMaio and Salcudean (2003a) first performed indentation, followed by needle insertion experiments on the phantom tissue, and captured global tissue deformation using cameras. The displacements of the markers were tracked using computer vision algorithms. Dual C-arm fluoroscopes and a CT scanner were used to calculate the dislocation of the fiducial markers in Hing et al. (2006) and Kerdok et al. (2003), respectively. The main limitation of this technique is that, placing markers on organs (either *in vivo* or *ex vivo*) is not practical. This is because use of markers in live organs might change the organ material properties and could possibly damage the organ. As opposed to using markers, Lau, Ramey, Corso, Thakor, and Hager (2004) implemented an algorithm to compute the surface geometry of beating pig heart in real time using the image intensity data. Other novel techniques that do not use markers to visualize the dynamic response of organs *in vivo* include attaching an ultrasound probe to the end of a robotically controlled laparoscopic tool (Leven et al., 2005) and using an air pressure and strobe system to provide an image of the deformed tissue in real time (Kaneko, Toya, & Okajima, 2007). Leven et al. (2005) tested their system on liver, while Kaneko et al. (2007) had designed their device to detect tumors in lungs. The technologies presented in Lau et al. (2004), Leven et al. (2005), and Kaneko et al. (2007) could be extended to measure tissue properties of organs *in vivo*.

As an alternative to the aforementioned global measurement techniques, elastography or elasticity imaging is a quantitative technique to map internal tissue elasticity. This is extremely useful in the interpretation of image data for physical modeling process. Several elastography techniques have been developed using imaging modalities such as ultrasound, CT, MRI, and optics, employing different tissue excitations, and extracting various parameters that provide a measure of tissue displacement (Ophir et al., 2002). Depending on the method of tissue deformation and parameters that are imaged, different terms are used to describe the images obtained, including strain, stress, velocity, amplitude, phase, vibration, compression, quasistatic, and functional images (Gao, Parker, Lerner, & Levinson, 1996). The underlying method for estimation of tissue properties is that the organ or tissue is loaded with an indentor and then, using imaging, it is possible to visualize the internal strain in the tissues (Tönuk & Silver-Thorn, 2003; Zhang, Zheng, & Mak, 1997). One of the fundamental deficiencies in using elastography for modeling tissues is that it is currently only possible to obtain Young's modulus and Poisson's ratio for the tissue, which are characteristics of linear elasticity. Turgay, Salcudean, and Rohling (2006) presented two methods to extract homogenous and inhomogeneous tissue properties while vibrating the tissue at a spectrum of frequencies and using an ultrasound probe to capture the tissue motion. They proposed two methods: modeling the tissues as a mass-spring-damper model and determining the transfer function from the tissue motion at two separate locations. The methods were able to determine the tissue properties for the homogenous tissue sample and only the middle layer of a inhomogeneous (layered) tissue sample.

As a result of the difficulties in measuring tissue properties *in vivo* with previously described methods, recent studies have also investigated methods for online estimation of local tissue properties during teleoperated surgical procedures. Most of the research done in this area is a subset of the work under environment property estimation during telemanipulation. Duchemin, Maillet, Poignet, Dombre, and Pierrot (2005) used a hybrid force/position controller for robotic telesurgery in skin harvesting procedures. With appropriate choice of gains, their controller estimated skin stiffness, friction, and thickness. Alternatively, De Gersem, Van Brussel, and Vander Sloten (2005) used a Kalman filtering technique to estimate the stiffness of soft materials during telemanipulation. Misra and Okamura (2006) proposed an indirect adaptive estimation algorithm for estimating tissue properties while palpating the tissue. With all these online estimation methods, the challenges associated with local and global measurement of tissue properties still exist.

7. Commercial Surgical Simulators

In addition to the published research on modeling tool-tissue interactions summarized in Table 1, there exist numerous commercial surgical simulators designed for the purpose of training clinicians. The methods employed by the companies for tissue modeling is not readily available, and there is extensive emphasis on producing models that are visually appealing. Further, in most commercially available simulators, tissue material parameters are tweaked based on qualitative evaluation performed by a few surgeons, rather than actual material testing.

Surgical simulators with force feedback provide an immersive environment for training and most commercially available simulators provide haptic feedback to the user. Reachin Technologies AB markets a simulator to train for cholecystectomy performed via laparoscopic surgery. In order to train surgeons for endoscopic, endourological, percutaneous access, laparoscopic surgery, and interventional endovascular procedures, Simbionix USA Corp. sells GI Mentor II™, URO Mentor™, PERC Mentor™, LAP Mentor™, and ANGIO Mentor™, respectively. Immersion Medical has developed numerous surgical simulation systems. The various training simulators include, CathSim® AccuTouch® (for vascular access and phlebotomy), Endoscopy AccuTouch® (for bronchoscopy and gastro-intestinal procedures),

Endovascular AccuTouch® (for percutaneous transluminal angioplasty and stenting procedures), Hysteroscopy AccuTouch® (for myomectomy and basic hysteroscopy skills), and Laparoscopy AccuTouch® (for laparoscopic abdominal procedures). Surgical Science Ltd. developed the LapSim system to train for abdominal keyhole surgery. ProMIS™, developed by Haptica Inc., is used to train for minimally invasive surgery techniques, while Mimic Technologies Inc. provides custom devices and software for the surgical simulation industry. Mentice AB has the Procedicus VIST™ (Vascular Intervention System Trainer), Procedicus VA™ (Virtual Arthroscopy), and Procedicus MIST™ (Minimally Invasive System Trainer), which are used for training in procedures, such as, cardiac catheterisation, shoulder and knee surgery, and laparoscopic cholecystectomy, respectively. Of these, only the Procedicus VA™ and Procedicus MIST™ do not provide force feedback to the users.

There exist several other commercially available surgical simulators that do not provide haptic feedback, but instead focus on training basic surgical skills (SurgicalSIM) or provide superior visualization capabilities (EYESI®). SurgicalSIM, developed by Medical Educational Technologies Inc., is used to train for general surgical tasks on anatomically accurate models based on patient's gender, size, and age. EYESI®, developed by VRmagic GmbH, is an ophthalmosurgical simulator that simulates stereo vision through the surgical microscope and allow tracking of tool motion. In addition to commercially available surgical simulators, research centers such as the Stanford University Medical Media and Information Technology develop simulators for hospitals, and Center for Integration of Medicine and Innovative Technology and National Capital Area Medical Simulation Center develop simulation technologies, primarily for defense-related medical treatments.

8. Discussion

This review paper provides an introduction to soft tissue modeling, with emphasis on the relevant continuum mechanics fundamentals and research to model surgical tool and tissue interactions for the purpose of building surgical simulators. We broadly split surgical tasks into non-invasive and invasive categories, and further divided the modeling techniques based on linear elasticity theory, nonlinear elasticity theory, and other methods. We also emphasized the use of accurate organ models by presenting some of the current methods to acquire realistic tissue properties via experiments. Our emphasis was on modeling methods that employed principles of continuum mechanics and used FE methods for simulation. A synopsis of the surveyed literature is provided in Table 1, and some of the commercially available surgical simulators are described in Section 7.

Based on our literature search, we observed that many researchers have done work in the area of modeling tool-tissue interactions using linear elasticity-based FE methods. However, few studies have been published using the more realistic nonlinear elasticity methods to model invasive tool-tissue interactions. Significant contributions have also been made using other non-standard modeling approaches. Such methods are primarily employed to enable simulations to run in real time, and in many cases accurate physics behind tissue deformation is not deemed a priority. It is still an open research question whether continuum mechanics-based FE approaches, meshless techniques, non-physics-based methods, or some combination of these is best method for simulating surgical tool and tissue interactions in real time. The constant challenge is to develop models that can appropriately and accurately describe the behavior of organs, yet are computationally efficient.

A fundamental, yet unanswered, research question is how much fidelity a surgical simulator needs in order to provide appropriate skill transfer to real procedures. There is some controversy over the relevance of haptic feedback and accurate tissue modeling for skill transfer, and rigorous, quantitative works needs to be done in this area (Ström et al., 2006). In contrast, for

surgical planning the required accuracy is determined by the clinical application. For example, in procedures like biopsies of the abdominal organs, breast, and lung tissue, predicting the location of the tumor as the needle penetrates the tissue is of primary importance, while reaching the target precisely in order to place radioactive seeds is paramount for procedures like prostate brachytherapy. The validation of surgical simulators is essential to motivate their application as a method for training and pre- and intra-operative planning. Validation techniques can be subjective (e.g. face and content validation) or objective (e.g. construct, concurrent, and predictive validation) (McDougall, 2007). If we follow the assumption that model fidelity and haptic feedback are important, then consider an approach in which we model the flow of information from the real tissue to acquired data, the model, the rendering technique, the haptic and/or visual display, and eventually the human user (Figure 12). We conjecture that each of these stages act as a "filter" in which information about force-motion relationships are lost or transformed. For example, the filter may be a result of the resolution of the measurement device used for gathering experimental data, the simulation model based on the constitutive law derived from experimental data, or simplification of the model required to perform real-time haptic rendering. In addition, haptic devices have their own dynamics and are affected by control issues such as sample-and-hold and quantization. Finally, the just noticeable difference of force perception of the human plays an vital role in quantifying the necessary fidelity of the simulation.

In order to accomplish surgical training and pre-operative planning using simulators that incorporate realistic tool-tissue interaction models along with haptic feedback, some significant challenges need to be overcome. The three main hurdles that need to be conquered are: First, the ability to obtain global responses of tool-tissue interactions *in vivo*; Second, formulating a methodology to incorporate this experimental data in a continuum mechanics framework to simulate realistic deformations of organs; and finally, making simplifications to the computational model such that the simulation runs in real time but does not compromise the effective realism of the tissue response. In spite of scientific challenges, this literature survey and trends over the past decade suggest that significant strides are being made by interdisciplinary research teams from the robotics, mechanics, graphics, and medicine communities to design surgical simulators and they hold great promise for training, practice, and patient-specific pre-operative planning.

Acknowledgments

References

ADINA R & D Inc. (1986). 71 Elton Avenue, Watertown, MA 02472 USA. (http://www.adina.com/)

Alterovitz, R.; Goldberg, K.; Pouliot, J.; Taschereau, R.; Hsu, CI. Needle insertion and radioactive seed implantation in human tissues: simulation and sensitivity analysis. Proc. IEEE Int'l. Conf. on Robotics and Automation; Taipei, Taiwan. 2003. p. 1793-1799.

ANSYS Inc. (1970). Southpointe, 275 Technology Drive, Canonsburg, PA 15317 USA. (http://www.ansys.com/)

Arruda EM, Boyce MC. Three-dimensional constitutive model for the large stretch behavior of rubber elastic materials. Journal of the Mechanics and Physics of Solids 1993;41(2):389–412.

Balaniuk, R.; Salisbury, K. Dynamic simulation of deformable objects using the long elements method. Proc. 10th Symposium on Haptic Interfaces for Virtual Environments and Teleoperator Systems; Orlando, USA. 2002. p. 58-65.

Basdogan C, Ho CH, Srinivasan MA. Virtual environments for medical training: Graphical and haptic simulation of laparoscopic common bile duct exploration. IEEE/ASME Trans Mechatronics 2001;6 (3):269–285.

Brett PN, Harrison AJ, Thomas TA. Schemes for the identification of tissue types and boundaries at the tool point for surgical needles. IEEE Trans Information Technology in Biomedicine 2000;4(1):30–36.

Brett PN, Parker TJ, Harrison AJ, Thomas TA, Carr A. Simulation of resistance forces acting on surgical needles. Proc Institution Mechanical Engineers, Part H: J Engineering in Medicine 1997;211(4):335–347.

Bro-Nielsen M. Finite element modeling in surgery simulation. Proc IEEE 1998;86(3):490–503.

Brouwer, I.; Ustin, J.; Bentley, L.; Sherman, A.; Dhruv, N.; Tendick, F. Medicine Meets Virtual Reality. Vol. 98. Amsterdam, the Netherlands: IOS Press; 2001. Measuring in vivo animal soft tissue properties for haptic modeling in surgical simulation; p. 69-74.

Brown, JD.; Rosen, J.; Sinanan, MN.; Hannaford, B. In vivo and postmortem compressive properties of porcine abdominal organs. 6th Int'l Conf. on Medical Image Computing and Computer Assisted Intervention (MICCAI); Berlin/Heidelberg, Germany: Springer; 2003. p. 238-245.

Carpue, JC. An account of two successful operations for restoring a lost nose. 1. Birmingham, USA: The Classics of Medicine Library; 1981.

Carter FJ, Frank TG, Davies PJ, McLean D, Cuschieri A. Measurements and modelling of the compliance of human and porcine organs. Medical Image Analysis 2001;5(4):213–236.

Castañeda, MAP.; Cosío, FA. Computer simulation of prostate resection for surgery training. Proc. Annual Int'l Conf. of the IEEE Engineering in Medicine and Biology; Cancun, Mexico. 2003. p. 1152-1155.

Center for Integration of Medicine and Innovative Technology. (1998). 165 Cambridge St., Suite 702, Boston, MA 02114 USA. (http://www.cimit.org/)

Chanthasopeephan T, Desai JP, Lau ACW. Measuring forces in liver cutting: new equipment and experimental results. Annals of Biomedical Engineering 2003;31(11):1372–1382. [PubMed: 14758928]

Chui C, Kobayashi E, Chen X, Hisada T, Sakuma I. Measuring forces in liver cutting: new equipment and experimental results. Medical and Biological Engineering and Computing 2004;42(6):787–798. [PubMed: 15587470]

COMSOL Inc. (1986). 1 New England Executive Park, Suite 350, Burlington, MA 01803 USA. (http://www.femlab.com/)

Cook, RD.; Malkus, DS.; Plesha, ME. Concepts and applications of finite element analysis. 3. New York, USA: John Wiley & Sons; 1989.

Cotin C, Delingette H, Ayache N. Real-time elastic deformations of soft tissues for surgery simulation. IEEE Trans Visualization and Computer Graphics 1999;5(1):62–73.

Cotin C, Delingette H, Ayache N. A hybrid elastic model for real-time cutting, deformations, and force feedback for surgery training and simulation. The Visual Computer 2000;16(8):437–452.

Crouch, JR.; Schneider, CM.; Wainer, J.; Okamura, AM. A velocity-dependent model for needle insertion in soft tissue. 8th Int'l Conf. on Medical Image Computing and Computer Assisted Intervention (MICCAI); Berlin/Heidelberg, Germany: Springer; 2005. p. 624-632.

d'Aulignac, D.; Balaniuk, R.; Laugier, C. A haptic interface for a virtual exam of the human thigh. Proc. IEEE Int'l. Conf. on Robotics and Automation; San Francisco, USA. 2000. p. 2452-2457.

d'Aulignac, D.; Laugier, C.; Cavusoglu, MC. Towards a realistic echographic simulator with force feedback. Proc. IEEE/RSJ Int'l. Conf. on Intelligent Robots and Systems; Kyongju, South Korea. 1999. p. 727-732.

Davies PJ, Carter FJ, Cuschieri A. Mathematical modelling for keyhole surgery simulations: A biomechanical model for spleen tissue. IMA Journal of Applied Mathematics 2002;67(1):41–67.

Davis, AB. Louis Thômas Jerome Auzoux and the papier mâché anatomical model. La Ceroplastica nella Scienza e nell'Arte: atti del I Congresso Internazionale Firenze; Florence, Italy. 1975. p. 257-279.

De S, Kim J, Lim YJ, Srinivasan MA. The point collocation-based method of finite spheres (pcmfs) for real time surgery simulation. Computers and Structures 2005;83(17–18):1515–1525.

De S, Lim YJ, Manivannan M, Srinivasan MA. Physically realistic virtual surgery using the point-associated finite field (paff) approach. Presence: Teleoperators & Virtual Environments 2006;15(3): 294–308.

De, S.; Srinivasan, MA. Medicine Meets Virtual Reality. Vol. 7. Amsterdam, the Netherlands: IOS Press; 1999. Thin walled models for haptic and graphical rendering of soft tissues in surgical simulators; p. 94-99.

De Gersem, G.; Van Brussel, H.; Vander Sloten, J. Enhanced haptic sensitivity for soft tissues using teleoperation with shaped impedance reflection. World Haptics Conf. (WHC); Pisa, Italy. 2005.

Delingette, H.; Subsol, G.; Cotin, S.; Pignon, J. A craniofacial surgery simulation testbed. Proc. 3rd Int'l. Conf. on Visualization in Biomedical Computing (VBC); Rochester, USA. 1994. p. 607-618.

Desai, CS.; Abel, JF. Introduction to the finite element method: a numerical method for engineering analysis. 1. Belmont, USA: Wadsworth Publishing Company; 1972.

DiMaio, SP.; Salcudean, SE. Simulated interactive needle insertion. Proc. 10th Symposium on Haptic Interfaces for Virtual Environments and Teleoperator Systems; Orlando, USA. 2002. p. 344-351.

DiMaio SP, Salcudean SE. Needle insertion modeling and simulation. IEEE Trans Robotics and Automation 2003a;19(5):864–875.

DiMaio, SP.; Salcudean, SE. Needle steering and model-based trajectory planning. 6th Int'l Conf. on Medical Image Computing and Computer Assisted Intervention (MICCAI); Berlin/Heidelberg, Germany: Springer; 2003b. p. 33-40.

DiMaio SP, Salcudean SE. Interactive simulation of needle insertion models. IEEE Trans Biomedical Engineering 2005;52(7):1167–1179.

Duchemin G, Maillet P, Poignet P, Dombre E, Pierrot F. A hybrid position/force control approach for identification of deformation models of skin and underlying tissues. IEEE Trans Biomedical Engineering 2005;52(2):160–170.

Eidgenössische Technische Hochschule. (n.d.). Institute of Mechanical Systems, CLA, Tannenstrasse 3, 8092 Zurich, Switzerland. (http://www.zfm.ethz.ch/e/biomechanics/)

Frank, AO.; Twombly, IA.; Barth, TJ.; Smith, JD. Finite element methods for real-time haptic feedback of soft-tissue models in virtual reality simulators. Proc. IEEE Virtual Reality Annual Int'l. Symposium (VRAIS); Yokohama, Japan. 2001. p. 257-263.

Fung YC. Biorheology of soft tissues. Biorheology 1973;10:139–155. [PubMed: 4728631]

Fung, YC. Biomechanics: mechanical properties of living tissues. 2. New York, USA: Springer-Verlag Inc; 1993.

Fung, YC.; Tong, P. Classical and computational solid mechannics. 1. Singapore: World Scientific Publishing Co. Pte. Ltd; 2001.

Gao L, Parker KJ, Lerner RM, Levinson SF. Imaging of the elastic properties of tissue-a review. Ultrasound in Medicine and Biology 1996;22(8):959–977. [PubMed: 9004420]

Georgia Tech-CASE Center. (n.d.). School of Civil & Environmental Engineering, Atlanta, GA 30332 USA. (http://www.gtstrudl.gatech.edu/)

Gibson, SF.; Mirtich, B. A survey of deformable modeling in computer graphics (Tech Rep No TR-97-19). Mitsubishi Electric Information Technology Center America; 1997. (http://www.merl.com)

Gladilin, E.; Zachow, S.; Deuflhard, P.; Hege, HC. A biomechanical model for soft tissue simulation in craniofacial surgery. Proc. Int'l Workshop on Medical Imaging and Augmented Reality; Hong Kong. 2001. p. 137-141.

Glozman, D.; Shoham, M. Flexible needle steering and optimal trajectory planning for percutaneous therapies. 7th Int'l Conf. on Medical Image Computing and Computer Assisted Intervention (MICCAI); Berlin/Heidelberg, Germany: Springer; 2004. p. 137-144.

Goksel, O.; Salcudean, SE.; DiMaio, SP.; Rohling, R.; Morris, J. 3d needle-yissue interaction simulation for prostate brachytherapy. 8th Int'l Conf. on Medical Image Computing and Computer Assisted Intervention (MICCAI); Berlin/Heidelberg, Germany: Springer; 2005. p. 827-834.

Gosline, AH.; Salcudean, SE.; Yan, J. Haptic simulation of linear elastic media with fluid pockets. Proc. 12th Symposium on Haptic Interfaces for Virtual Environments and Teleoperator Systems; Chicago, USA. 2004. p. 266-271.

Haptica Inc. (n.d.). 101 Federal Street, Suite 1900, Boston, MA 02110 USA. (http://www.haptica.com/)

Harders, M.; Bajka, M.; Spaelter, U.; Tuchschmidi, S.; Bleuler, H.; Székely, G. Highly-realistic, immersive training environment for hysteroscopy. In: JDW, et al., editors. Medicine meets virtual reality. Vol. 119. Amsterdam: IOS Press; 2006. p. 176-181.

Hing, JT.; Brooks, AD.; Desai, JP. Reality-based needle insertion simulation for haptic feedback in prostate brachytherapy. Proc. IEEE Int'l. Conf. on Robotics and Automation; Orlando, USA. 2006. p. 619-624.

Holzapfel, GA. Nonlinear solid mechanics: a continuum approach for engineering. 1. Chichester, UK: John Wiley & Sons, Ltd; 2000.

Hu, T.; Desai, JP. A biomechanical model of the liver for reality-based haptic feedback. 6th Int'l Conf. on Medical Image Computing and Computer Assisted Intervention (MICCAI); Berlin/Heidelberg, Germany: Springer; 2003. p. 75-82.

Hu, T.; Desai, JP. Characterization of soft-tissue material properties: large deformation analysis. In: Cotin, S.; Metaxas, DN., editors. Proc Int'l Symposium Medical Simulation (ISMS); Berlin/Heidelberg, Germany: Springer; 2004. p. 28-37.

Hutter R, Schmitt KU, Niederer P. Mechanical modeling of soft biological tissues for application in virtual reality based laparoscopy simulators. Technology and Health Care 2000;8:15–24. [PubMed: 10942988]

Immersion Medical. (2000). 55 West Watkins Mill Road, Gaithersburg, MD 20878 USA. (http://www.immersion.com/medical)

Institut National de Recherche en Informatique et en Automatique. (n.d.). Virtual Reality Platform, Rhône-Alpes, Inovallée, 655 avenue de l'Europe, Montbonnot, 38 334 Saint Ismier Cedex, France. (http://www.inrialpes.fr/sed/PRV/)

James D, Pai DK. A unified treatment of elastostatic contact simulation for real time haptics. Haptics-e 2001;2(1):1–13.

Kaneko, M.; Toya, C.; Okajima, M. Active strobe imager for visualizing dynamic behavior of tumors. Proc. IEEE Int'l. Conf. on Robotics and Automation; Rome, Italy. 2007. p. 3009-3014.

Keeve, E.; Girod, S.; Girod, B. Craniofacial surgery simulation. Proc. 4th Int'l. Conf. on Visualization in Biomedical Computing (VBC); Hamburg, Germany. 1996. p. 541-546.

Kerdok AE, Cotin SM, Ottensmeyer MP, Galea AM, Howe RD, Dawson SL. Truth cube: Establishing physical standards for soft tissue simulation. Medical Image Analysis 2003;7(3):283–291. [PubMed: 12946469]

Kim, J.; Srinivasan, MA. Characterization of visoelastic soft tissue properties from in vivo animal experiments and inverse fe parameter characterization. 8th Int'l Conf. on Medical Image Computing and Computer Assisted Intervention (MICCAI); Berlin/Heidelberg, Germany: Springer; 2005. p. 599-606.

Kim, J.; Tay, BK.; Stylopoulos, N.; Rattner, DW.; Srinivasan, MA. Characterization of intra-abdominal tissues from in vivo animal experiments for surgical simulation. 6th Int'l Conf. on Medical Image Computing and Computer Assisted Intervention (MICCAI); Berlin/Heidelberg, Germany: Springer; 2003. p. 206-213.

Koch, RM.; Gross, MH.; Carls, FR.; Buren, DF.; von Fankhauser, GH.; Parish, YI. Simulating facial surgery using finite element models; New Orleans, USA: 1996. p. 421-428.

Kühnapfel U, Çakmak HK, Maaß H. Endoscopic surgery training using virtual reality and deformable tissue simulation. Computers and Graphics 2000;24(5):671–682.

Kyung, K-K.; Kwon, D-S.; Kwon, S-M.; Kang, H-S.; Ra, JB. Force feedback for a spine biopsy simulator with volume graphic model. Proc. IEEE/RSJ Int'l. Conf. on Intelligent Robots and Systems; Maui, USA. 2001. p. 1732-1737.

Lang J, Pai DK, Woodham RJ. Acquisition of elastic models for interactive simulation. Int'l J Robotics Research 2002;21(8):713–734.

Lau, WW.; Ramey, NA.; Corso, JJ.; Thakor, NV.; Hager, GD. Stereo-based endoscopic tracking of cardiac surface deformation. 7th Int'l Conf. on Medical Image Computing and Computer Assisted Intervention (MICCAI); Berlin/Heidelberg, Germany: Springer; 2004. p. 494-501.

Lawrence Livermore National Laboratory. (1970). Methods Development Group, 7000 East Avenue, Livermore, CA 94550 USA. (http://www-eng.llnl.gov/mdg/mdgcodes dyna3d.html)

Leven, J.; Burschka, D.; Kumar, R.; Zhang, G.; Blumenkranz, S.; Dai, X., et al. Davinci canvas: a telerobotic surgical system with integrated robot-assisted, laproscopic ultrasound capability. 8th Int'l Conf. on Medical Image Computing and Computer Assisted Intervention (MICCAI); Berlin/Heidelberg, Germany: Springer; 2005. p. 811-818.

Liu A, Tendick F, Cleary K, Kaufmann C. A survey of surgical simulation: applications, technology, and education. Presence: Teleoperators & Virtual Environments 2003;12(6):599–614.

Liu, Y.; Kerdok, AE.; Howe, RD. A nonlinear finite element model of soft tissue indentation. In: Cotin, S.; Metaxas, DN., editors. Proc Int'l symposium Medical Simulation (ISMS). Vol. 3078. Berlin/Heidelberg, Germany: Springer; 2004. p. 67-76.

Mahvash M, Hayward V. Haptic rendering of cutting: a fracture mechanics approach. Haptics-e 2001;2(3):1–12.

Mahvash, M.; Hayward, V.; Lloyd, JE. Haptic rendering of tool contact. Proc. Eurohaptics; Edinburgh, Scotland. 2002. p. 110-115.

Mahvash, M.; Okamura, AM. A fracture mechanics approach to haptic synthesis of tissue cutting with scissors. First Joint Eurohaptics Conf. and Symposium on Haptic Interfaces for Virtual Environment and Teleoperator Systems (WHC); Pisa, Italy. 2005. p. 356-362.

Mahvash M, Voo L, Kim D, Jeung K, Okamura AM. Modeling the forces of cutting with scissors. IEEE Trans Biomedical Engineering. 2007 (In Press: IEEE Trans. Robotics).

McDougall EM. Validation of surgical simulators. J Endourology 2007;21(3):244–247.

Medical Educational Technologies Inc. (1996). 6000 Fruitville Road, Sarasota, FL 34232 USA. (http://www.meti.com/)

Mentice AB. (1999). Rosenlundsgatan 8, 411 20 Göteborg, Sweden. (http://www.mentice.com/)

Miller K. Biomechanics of soft tissues. Medical Science Monitor 2000;6(1):158–167. [PubMed: 11208305]

Miller K, Chinzei K. Mechanical properties of brain tissue in tension. J Biomechanics 2002;35(4):483–490.

Mimic Technologies Inc. (2001). 119 1st Ave South, Suite 360, Seattle 98104 USA. (http://www.mimic.ws/)

Misra, S.; Okamura, AM. Environment parameter estimation during bilateral telemanipulation. Proc. 14th Symposium on Haptic Interfaces for Virtual Environments and Teleoperator Systems; Alexandria, USA. 2006. p. 301-307.

Misra, S.; Ramesh, KT.; Okamura, AM. Medicine Meets Virtual Reality. Vol. 132. Amsterdam, the Netherlands: IOS Press; 2008. Physically valid surgical simulators: linear versus nonlinear tissue models; p. 293-295.

Molinari E, Fato M, Leo GD, Riccardo D, Beltrame F. Simulation of the biomechanical behavior of the skin in virtual surgical applications by finite element method. IEEE Trans Biomedical Engineering 2005;52(9):1514–1521.

MSC Software Corp. (1963). 2 MacArthur Place, Santa Ana, CA 92707 USA. (http://www.mscsoftware.com/)

National Capital Area Medical Simulation Center. (n.d.). Uniformed Services University, 4301 Jones Bridge Road, Bethesda, MD 20814 USA. (http://simcen.usuhs.mil/)

Nava, A.; Mazza, E.; Haefner, O.; Bajka, M. Experimental observation and modelling of preconditioning in soft biological tissues. 2nd Int'l Symposium on Medical Simulation; Cambridge, USA. 2004. p. 1-9.(http://www.medicalsim.org/symposium2004/)

Nienhuys, H-W.; van der Stappen, FA. A computational technique for interactive needle insertions in 3d nonlinear material. Proc. IEEE Int'l. Conf. on Robotics and Automation; New Orleans, USA. 2004. p. 2061-2067.

Ogden, RW. Non-linear elastic deformations. 1. Chichester, UK: Ellis Horwood Ltd; 1984.

Okamura AM, Simone C, O'Leary MD. Force modeling for needle insertion into soft tissue. IEEE Trans Biomedical Engineering 2004;51(10):1707–1716.

Okamura, AM.; Webster, RJ., III; Nolin, JT.; Johnson, KW.; Jafry, H. The haptic scissors: cutting in virtual environments. Proc. IEEE Int'l. Conf. on Robotics and Automation; Taipei, Taiwan. 2003. p. 828-833.

Ophir J, Alam SK, Garra BS, Kallel F, Konofagou EE, Krousko T, et al. Elastography: imaging the elastic properties of soft tissues with ultrasound. J Medical Ultrasonics 2002;29(4):155–171.

Ottensmeyer MP. Tempest i-d: an instrument for measuring solid organ soft tissue properties. Experimental Techniques 2002;26(3):48–50.

Ottensmeyer, MP.; Kerdok, AE.; Howe, RD.; Dawson, SL. The effects of testing environment on the viscoelastic properties of soft tissues. In: Cotin, S.; Metaxas, DN., editors. Proc Medical Simulation: Int'l Symposium (ISMS). Vol. 3078. Berlin/Heidelberg, Germany: Springer; 2004. p. 9-18.

Picinbono G, Delingette H, Ayache N. Non-linear anisotropic elasticity for real-time surgery simulation. Graphical Models 2003;65(5):305–321.

Picinbono, G.; Lombardo, J-C.; Delingette, H.; Ayache, N. Anisotropic elasticity and force extrapolation to improve realism of surgery simulation. Proc. IEEE Int'l. Conf. on Robotics and Automation; San Francisco, USA. 2000. p. 596-602.

Popa, DO.; Singh, SK. Creating realistic force sensations in a virtual environment: experimental system, fundamental issues and results. Proc. IEEE Int'l. Conf. on Robotics and Automation; Leuven, Belgium. 1998. p. 59-64.

Puso MA, Weiss JA. Finite element implementation of anisotropic quasi-linear viscoelasticity using a discrete spectrum approximation. ASME J Biomechanical Engineering 1998;120(1):62–70.

Reachin Technologies AB. (1997). Årstaängsvägen 24, 117 43 Stockholm, Sweden. (http://www.reachin.se/)

Roberts JC, Merkle AC, Biermann PJ, Ward EE, Carkhuff BG, Cain RP, et al. Computational and experimental models of the human torso for non-penetrating ballistic impact. J Biomechanics 2007;40(1):125–136.

Sacred Heart Medical Center. (2004). 1255 Hilyard Street, Eugene, OR 97401 USA. (http://www.peacehealth.org/OHVI/CardiacSurgery.htm)

Sagar, MA.; Bullivant, D.; Mallinson, GD.; Hunter, PJ.; Hunter, IW. A virtual environment and model of the eye for surgical simulation. Proc. 21st Annual Conf. on Computer Graphics and Interactive Techniques (SIGGRAPH); Orlando, USA. 1994. p. 205-212.

Satava RM. Accomplishments and challenges of surgical simulation. Surgical Endoscopy 2001;15(3): 232–241. [PubMed: 11344421]

Sedef, M.; Samur, E.; Basdogan, C. Visual and haptic simulation of linear viscoelastic tissue behaviour based on experimental data. Proc. 14th Symposium on Haptic Interfaces for Virtual Environments and Teleoperator Systems; Alexandria, USA. 2006. p. 201-208.

SensAble Technologies Inc. (1990). 15 Constitution Way, Woburn, MA 01801 USA. (http://www.sensable.com/haptic-phantom-omni.htm)

Siemens PLM Software. (n.d.). 5800 Granite Parkway, Suite 600, Plano, TX 75024 USA. (http://www.plm.automation.siemens.com/)

Simbionix USA Corp. (1997). 11000 Cedar Ave., Suite 210, Cleveland, OH 44106 USA. (http://www.simbionix.com/)

Simulia. (1981). Rising Sun Mills, 166 Valley Street, Providence, RI 02909 USA. (http://www.simulia.com/)

Spencer, AJM. Deformations of fibre-reinforced materials. 1. Oxford, UK: Clarendon Press; 1972.

Stanford University Medical Media and Information Technology. (n.d.). 251 Campus Drive, MSOB-2nd Floor, MC:5466, Stanford, CA 94305 USA. (http://summit.stanford.edu/)

Ström P, Hedman L, Särnå L, Kjellin A, Wredmark T, Felländer-Tsai L. Early exposure to haptic feedback enhances performance in surgical simulator training: a prospective randomized crossover study in surgical residents. Surgical Endoscopy 2006;20(9):1383–1388. [PubMed: 16823652]

Sundaraj, K.; Mendoza, C.; Laugier, C. A fast method to simulate virtual deformable objects with force feedback. 7th Int'l Conf. on Automation, Robotics, Control, and Vision (ICARCV); Singapore. 2002. p. 413-418.

Surgical Science Ltd. (1995). Haraldsgatan 5, SE 413 14 Göteborg, Sweden. (http://www.surgical-science.com/)

Székely G, Brechbühler C, Dual J, Enzler R, Hug J, Hutter R, et al. Virtual reality-based simulation of endoscopic surgery. Presence: Teleoperators & Virtual Environments 2000;9(3):310–333.

Tendick F, Downes M, Goktekin T, Cavusoglu MC, Feygin D, Wu X. A virtual environment testbed for training laproscopic surgical skills. Presence: Teleoperators & Virtual Environments 2000;9(3): 236–255.

Tönuk E, Silver-Thorn B. Nonlinear elastic material property estimation of lower extremity residual limb tissues. IEEE Trans Neural Systems and Rehabilitation Engineering 2003;11(1):43–53.

Turgay E, Salcudean S, Rohling R. Identifying the mechanical properties of tissue by ultrasound strain imaging. Ultrasound in Medicine and Biology 2006;32(2):221–235. [PubMed: 16464668]

VRmagic GmbH. (n.d.). Augustaanlage 32, 68165 Mannheim, Germany. (http://www.vrmagic.com/)

Vuskovic, V.; Kauer, M.; Székely, G.; Reidy, M. Realistic force feedback for virtual reality based diagnostic surgery simulators. Proc. IEEE Int'l. Conf. on Robotics and Automation; San Francisco, USA. 2000. p. 1592-1598.

Wang, X.; Fenster, A. A virtual reality based 3d real-time interactive brachytherapy simulation of needle insertion and seed implantation. IEEE Int'l Symposium on Biomedical Imaging: From Nano to Macro; Arlington, USA. 2004. p. 280-283.

Waters K. Physical model of facial tissue and muscle articulation derived from computer tomography data. Proc SPIE-The International Society for Optical Engineering 1992;1808:574–583.

Wu W, Heng PA. An improved scheme of an interactive finite element model for 3d soft-tissue cutting and deformation. The Visual Computer 2005;21(8–10):707–716.

Wu X, Downes MS, Goktekin T, Tendick F. Adaptive nonlinear finite elements for deformable body simulation using dynamic progressive meshes. Computer Graphics Forum 2001;20(3):349–358.

Yamada, H. Strength of biological materials. 1. Baltimore, USA: The Williams & Wilkins Company; 1970.

Zhang M, Zheng YP, Mak AF. Estimating the effective young's modulus of soft tissues from indentation tests–nonlinear finite element analysis of effects of friction and large deformation. Medical Engineering & Physics 1997;19(6):512–517. [PubMed: 9394898]

Zhukov, L.; Barr, AH. Heart-muscle fiber reconstruction from diffusion tensor mri. Proc. IEEE Visualization Conf.; Seattle, USA. 2003. p. 597-602.

Zienkiewicz, OC.; Taylor, RL.; Zhu, JZ. The finite element method: its basis and fundamentals. 6. Oxford, UK: Elsevier Butterworth-Heinemann; 2005.
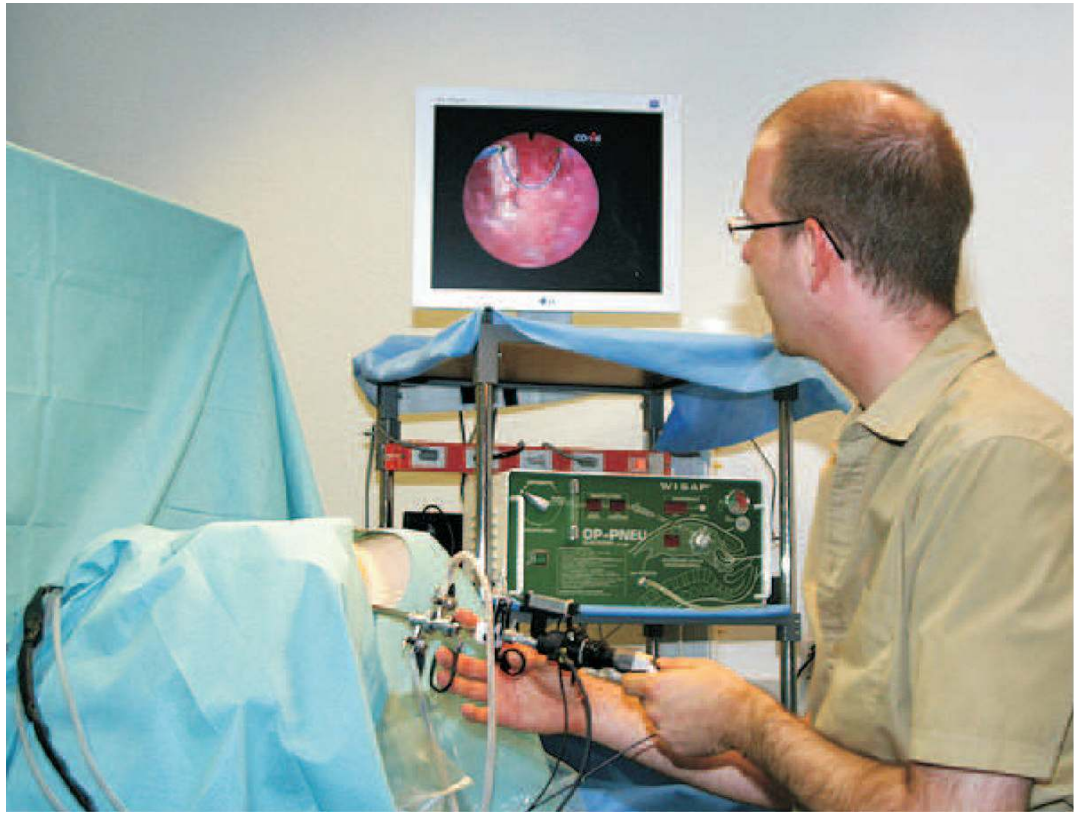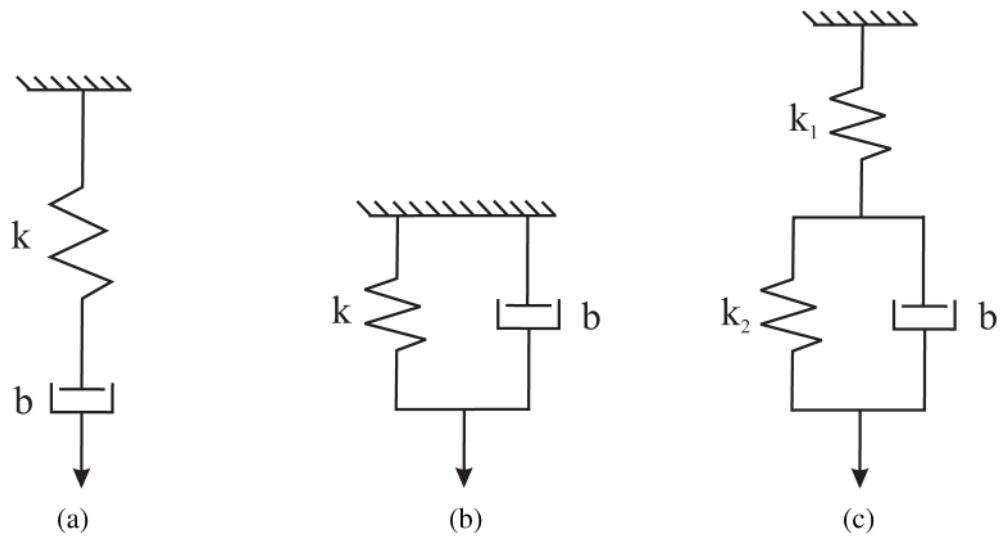
Figure 1.
Hysteroscopy training simulation environment coupled with a haptic device (Harders et al., 2006). *Reprinted from Studies in Health Technology and Informatics, Vol. 119, Harders et al. Highly-realistic, immersive training environment for hysteroscopy, pp. 176–181, ©(2006), with permission from IOS Press.*
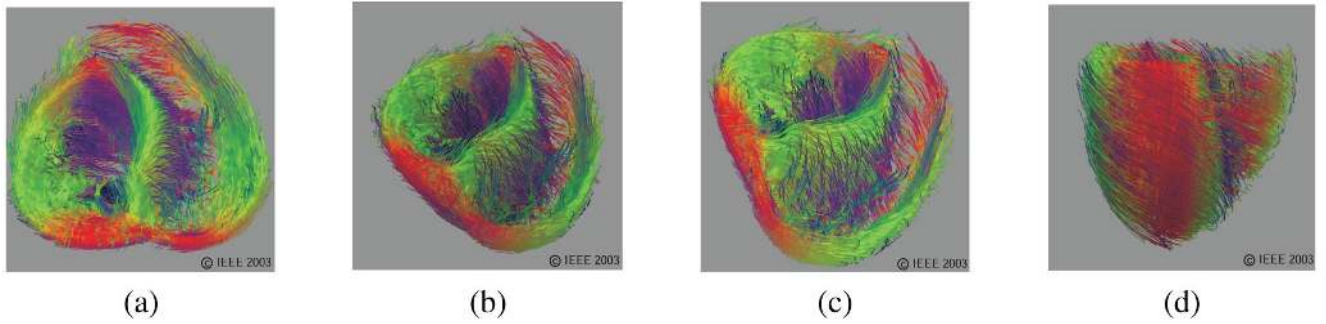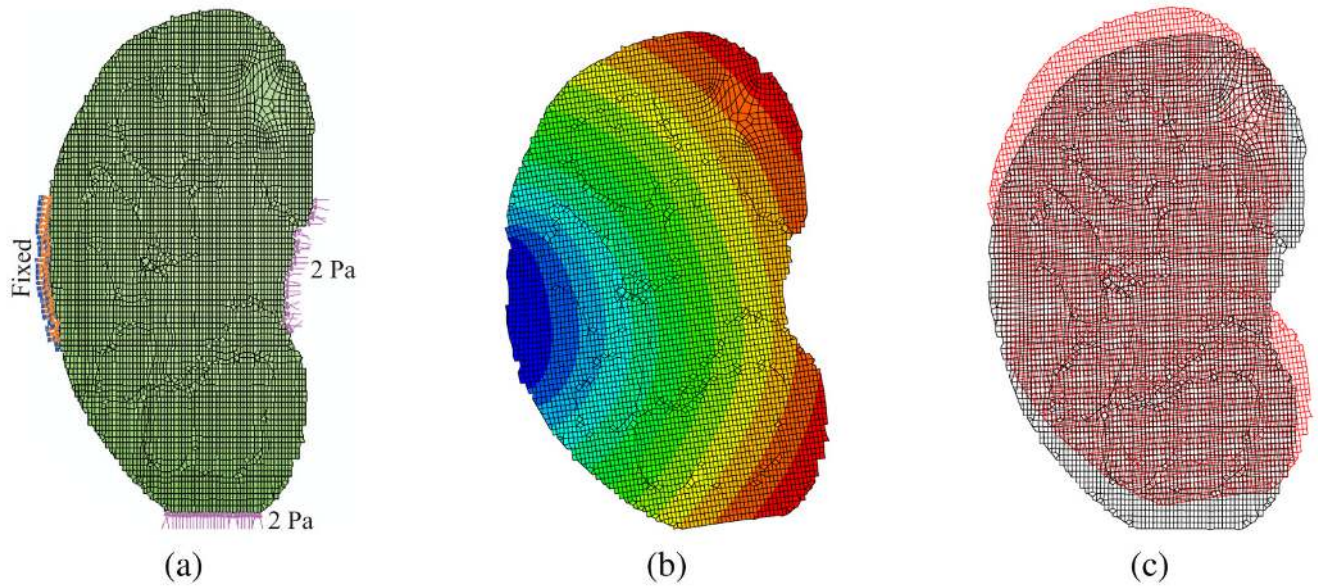
Figure 2.
Tissue fiber orientation of the heart on the inside surface, (a) and (b), and outside surface, (c) and (d), constructed using diffusion tensor imaging (Zhukov & Barr, 2003). *Images are printed with permission from ©IEEE 2003.*
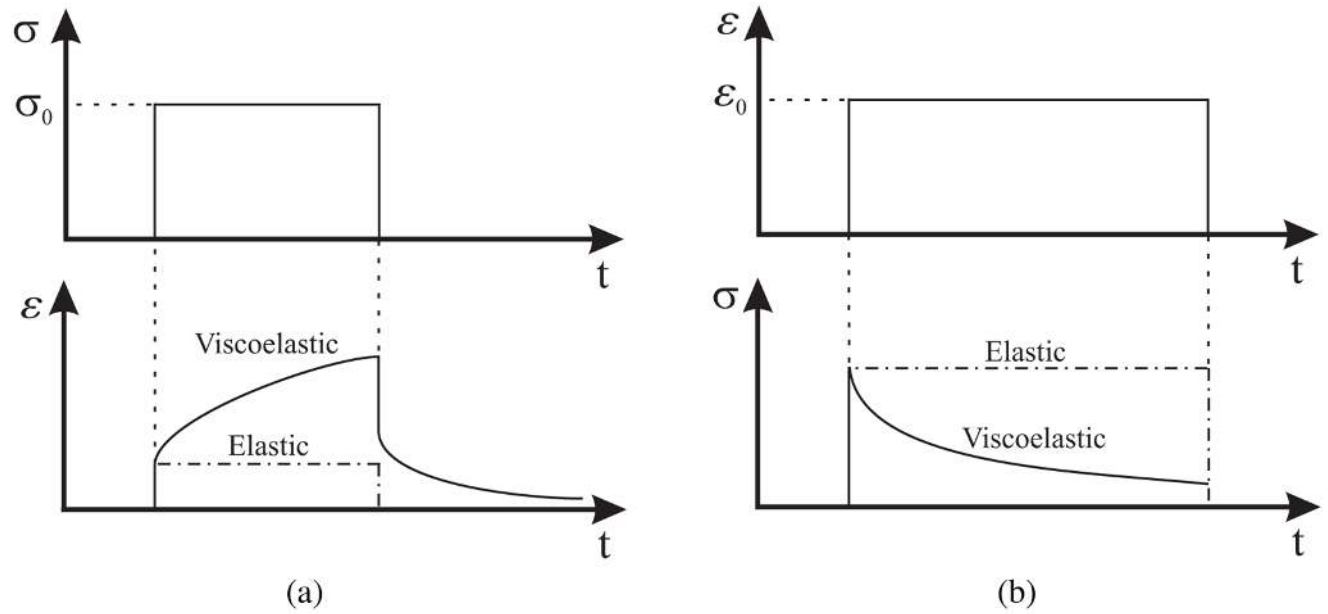
Figure 3.
Examples of characteristic properties of viscoelastic materials (a) creep and creep recovery - for a constant applied shear stress σ_0 results in an increase in shear strain (b) stress relaxation - for a constant applied shear strain ε_0 results in a decrease in shear stress until it reaches a steady state value.

Figure 4.
Standard viscoelastic models commonly used to represent soft tissues (a) Maxwell (b) Kelvin-Voigt (or Voigt) (c) Zener standard linear solid (or Kelvin) (Fung, 1993).

Figure 5.
Two-dimensional ABAQUS simulation results for soft tissue deformation of the human kidney that incorporates a hyperelastic constitutive model (Mooney-Rivlin model: C_{10} = 682.31 Pa and C_{01} = 700.02 Pa (Kim & Srinivasan, 2005)) and the left side boundary nodes are fixed, while loads are applied at the bottom and right edge nodes (a) undeformed mesh (b) contour plot of displacements (c) undeformed mesh is black, while deformed mesh is red.
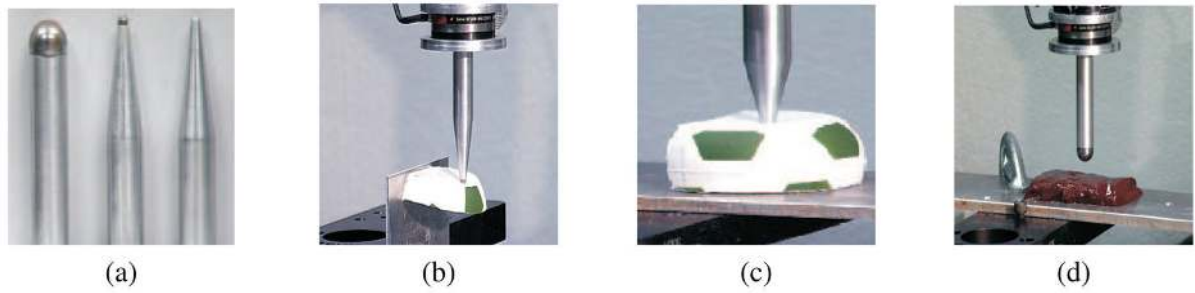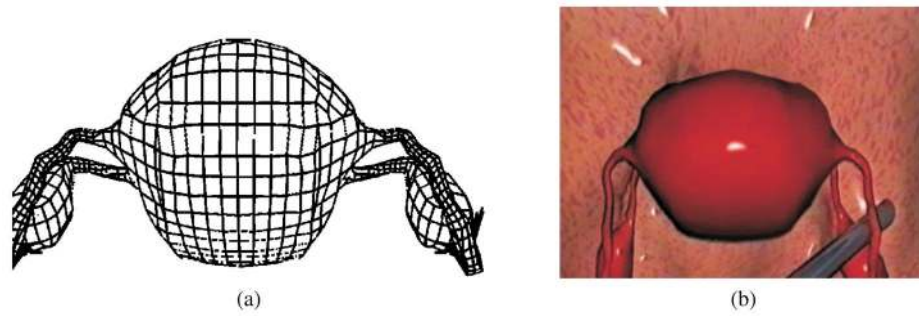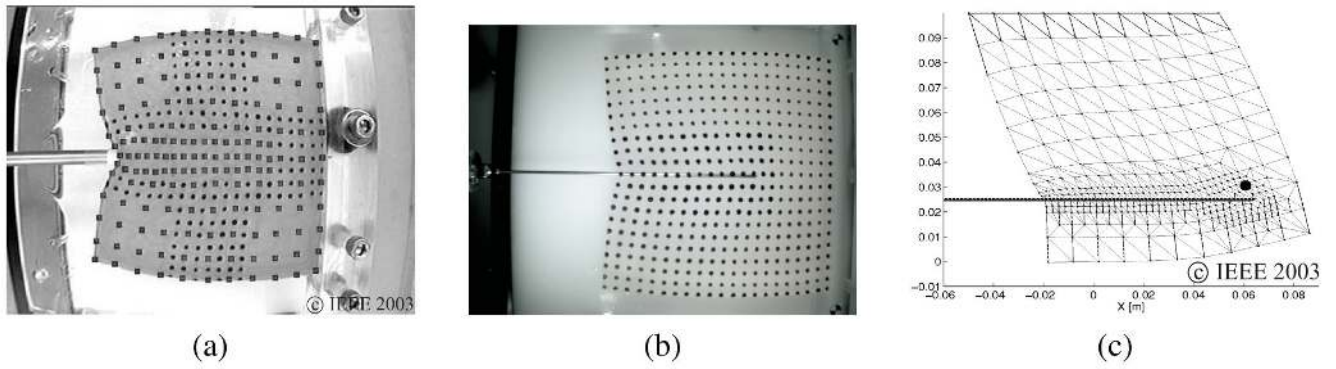
Figure 6.
(a) Tools tested and measuring tool-material interaction forces during (b) and (c) deformation of rubber (d) deformation of bovine liver (Mahvash et al., 2002). *Images printed with permission from publisher (EuroHaptics 2002).*
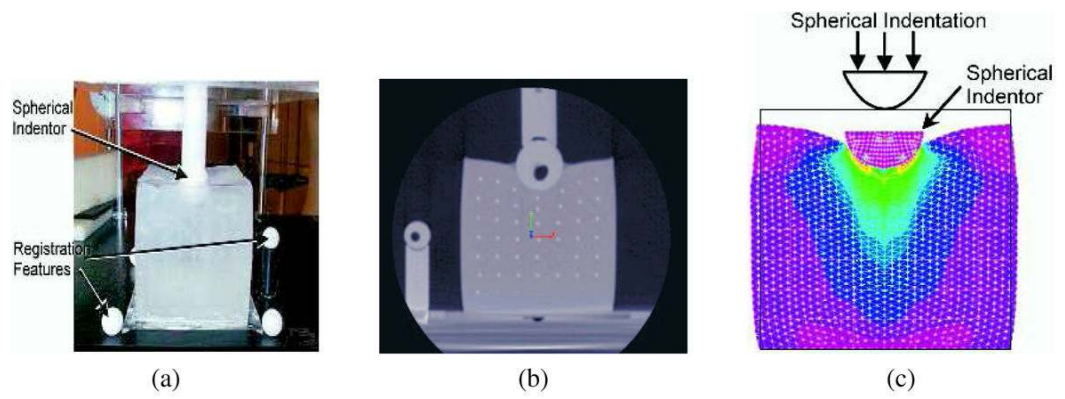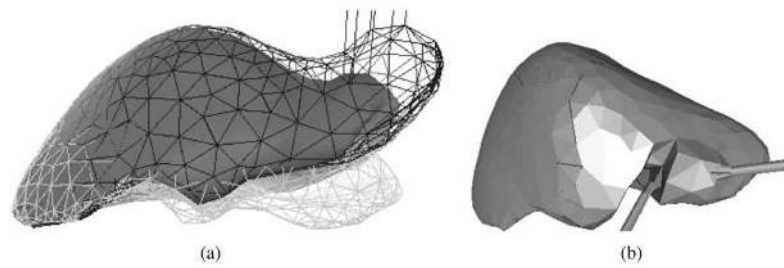
Figure 7.
Indentation test on the "Truth Cube" embedded with fiducials (a) experimental test setup (b) CT of center vertical slice under 22% strain (c) FE model under 22% strain (Kerdok et al., 2003). *Images printed with permission from Copyright ©2003 Elsevier B.V.*

Figure 8.
Formulation and results of the endoscopic simulator: (a) FE model of the human uterus containing 2000 elements. (b) Tool-tissue interaction model used in the surgical simulator (Székely et al., 2000). *Images printed with permission from MIT Press Journals ©2000 by the Massachusetts Institute of Technology*.
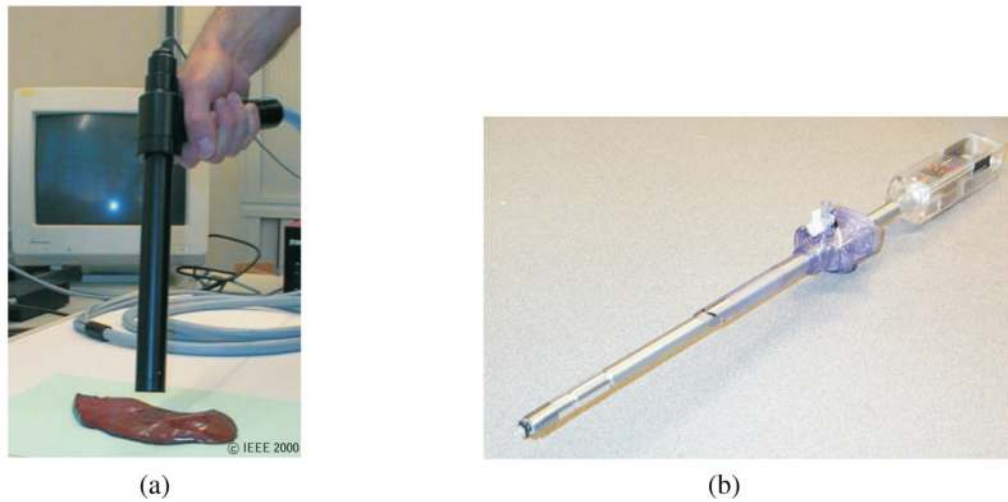
Figure 9.
Needle insertion and simulation modeling: (a) Probing for estimation of material properties of phantom tissue. (b) 17 gauge epidural needle inserted into phantom tissue while motion of markers and insertion forces are recorded. (c) FE simulation of needle insertion with small target embedded within elastic tissue (DiMaio & Salcudean, 2003a). *Images printed with permission from ©IEEE 2003*.
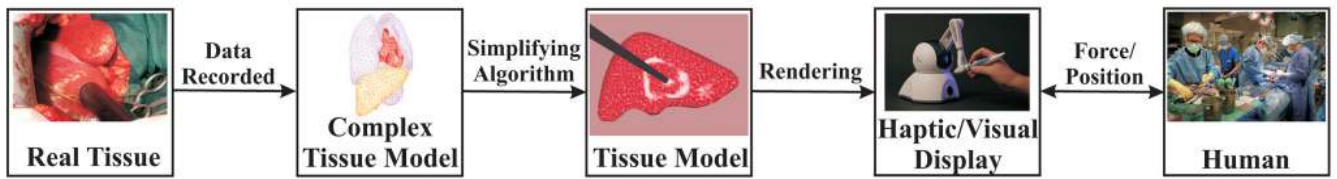
Figure 10.
Results from work presented in Picinbono et al. (2003): (a) Comparison between linear (wireframe) versus nonlinear (solid) elasticity-based models for same force applied to right lobe of the liver; the linear model undergoes large unrealistic deformation. (b) Simulating hepatic resection using a nonlinear anisotropic model. *Images printed with permission from Copyright ©2003 Elsevier Science (USA).*

(a)

(b)

Figure 11.
Devices used to measure tissue properties *in vivo*: (a) Tissue aspiration technique (Vuskovic et al., 2000). *Image printed with permission from ©IEEE 2000.* (b) TeMPeST 1-D with 12 mm surgical port (Ottensmeyer, 2002). *Image printed with permission from Wiley-Blackwell Publishing Ltd.*

Figure 12.
Modeling the information flow in simulator development and application. Each stage acts as a "filter" in which information about force-motion relationships are lost or transformed. *Images are obtained from* Roberts et al. (2007), *Eidgenössische Technische Hochschule,* Sacred Heart Medical Center (2004), SensAble Technologies Inc. (1990), *and Institut National de Recherche en Informatique et en Automatique. Image corresponding to* Roberts et al. (2007) *printed with permission from Copyright ©2007 Elsevier Ltd.*

Table 1

Survey of tool-tissue interaction models for surgical simulation and robot-assisted surgery. Within each category, authors are listed alphabetically and simulators that provide haptic feedback are designated by †.

Operation	Model			
	Linear elastic FE	**Hyperelastic FE**	**Visco-hyperelastic FE**	**Other methods**
Deformation (via indentation)	*Simulation only*			
	Basdogan et al. †	Y. Liu et al.	Puso and Weiss	LEM (2002LEM (2002) †
	Bro-Nielsen	X. Wu et al.		Mass- (1994; 1996; 1996)
	Cotin et al. †			spring- (2003 (1992)
	Frank, Twombly, Barth, and Smith			damper model (2000)
	Gladilin et al.			Thin-walled model (1999)
	Kühnapfel et al. †			PCMFS (2005) †and PAFF (2006) †
				BEM solution (2001)
				J-shaped function (1994)
	Real/Phantom tissue studies			
	Gosline et al. †	Carter et al.	Székely et al. †	Curve-fitting (2003)
	Kerdok et al.	Chui et al.		Green's function (2002)
	Sedef et al.-	Davies et al.	Miller	
	viscoelastic	Hu and Desai	Nava et al.	
		Molinari et al.	Kim et al.	
Rupture (via needle insertion)	*Simulation only*			
	Alterovitz et al.	Nienhuys and van der Stappen		Spring model (2004)
				Volume model (2001)
				3D chain mail (2004)
	Real/Phantom tissue studies			
	Crouch et al.			Resistive-(1997) †
	DiMaio and Salcudean †			force model (2000) †
	Hing et al.			Curve-fitting (2001)
				Friction model (2004)

Operation	Model			
	Linear elastic FE	**Hyperelastic FE**	**Visco-hyperelastic FE**	**Other methods**
Cutting (via blade/scissors)	*Simulation only*			
	Picinbono et al. †	Picinbono et al.		Hybrid model (2000)
	W. Wu and Heng			
	Real/Phantom tissue studies			
	Chanthasopeephan et al.			Fracture mechanics (2001)
				Haptic Scissors (2003)